

# *Arabidopsis* ROCK1 transports UDP-GlcNAc/UDP-GalNAc and regulates ER protein quality control and cytokinin activity

Michael C. E. Niemann<sup>a</sup>, Isabel Bartrina<sup>a</sup>, Angel Ashikov<sup>b</sup>, Henriette Weber<sup>a</sup>, Ondřej Novák<sup>c</sup>, Lukáš Spíchal<sup>c</sup>, Miroslav Strnad<sup>c</sup>, Richard Strasser<sup>d</sup>, Hans Bakker<sup>b</sup>, Thomas Schmülling<sup>a</sup>, and Tomáš Werner<sup>a,1</sup>

<sup>a</sup>Institute of Biology/Applied Genetics, Dahlem Centre of Plant Sciences, Freie Universität Berlin, D-14195 Berlin, Germany; <sup>b</sup>Department of Cellular Chemistry, Hannover Medical School, D-30625 Hannover, Germany; <sup>c</sup>Laboratory of Growth Regulators and Department of Chemical Biology and Genetics, Centre of the Region Haná for Biotechnological and Agricultural Research, Palacký University and Institute of Experimental Botany, Academy of Sciences of the Czech Republic, CZ-78371, Olomouc, Czech Republic; and <sup>d</sup>Department of Applied Genetics and Cell Biology, University of Natural Resources and Life Sciences, 1190 Vienna, Austria

Edited by Natasha V. Raikhel, Center for Plant Cell Biology, Riverside, CA, and approved December 2, 2014 (received for review October 7, 2014)

The formation of glycoconjugates depends on nucleotide sugars, which serve as donor substrates for glycosyltransferases in the lumen of Golgi vesicles and the endoplasmic reticulum (ER). Import of nucleotide sugars from the cytosol is an important prerequisite for these reactions and is mediated by nucleotide sugar transporters. Here, we report the identification of REPRESSOR OF CYTOKININ DEFICIENCY 1 (ROCK1, At5g65000) as an ER-localized facilitator of UDP-*N*-acetylglucosamine (UDP-GlcNAc) and UDP-*N*-acetylgalactosamine (UDP-GalNAc) transport in *Arabidopsis thaliana*. Mutant alleles of *ROCK1* suppress phenotypes inferred by a reduced concentration of the plant hormone cytokinin. This suppression is caused by the loss of activity of cytokinin-degrading enzymes, cytokinin oxidases/dehydrogenases (CKXs). Cytokinin plays an essential role in regulating shoot apical meristem (SAM) activity and shoot architecture. We show that *rock1* enhances SAM activity and organ formation rate, demonstrating an important role of ROCK1 in regulating the cytokinin signal in the meristematic cells through modulating activity of CKX proteins. Intriguingly, genetic and molecular analysis indicated that *N*-glycosylation of CKX1 was not affected by the lack of ROCK1-mediated supply of UDP-GlcNAc. In contrast, we show that CKX1 stability is regulated in a proteasome-dependent manner and that ROCK1 regulates the CKX1 level. The increased unfolded protein response in *rock1* plants and suppression of phenotypes caused by the defective brassinosteroid receptor *bri1-9* strongly suggest that the ROCK1 activity is an important part of the ER quality control system, which determines the fate of aberrant proteins in the secretory pathway.

ROCK1 | cytokinin | CKX | shoot meristem | nucleotide sugars

The biosynthesis of glycans and glycoconjugates (e.g., glycoproteins or glycolipids) requires glycosyltransferases residing in the Golgi apparatus and endoplasmic reticulum (ER). Their activity depends on the presence of activated monosaccharide donor substrates, nucleotide sugars. About 30 different nucleotide sugars have been detected in plants, most of which are synthesized in the cytosol and required to be selectively transported over the compartmental membrane (1). This transport is mediated by nucleotide sugar transporters (NSTs), which generally function as antiporters transporting nucleotide sugars usually in exchange to the corresponding nucleoside monophosphate across the membranes of ER and Golgi (2). They belong to the NST/triosephosphate translocator family consisting of 40 members in *Arabidopsis* (3). Transported substrates have been previously identified for 13 NSTs in *Arabidopsis*, which include UDP-glucose (UDP-Glc), UDP-galactose (UDP-Gal), GDP-mannose (GDP-Man), and CMP-sialic acid (4–8). However, molecular mechanisms underlying transport of other nucleotide sugars in plants are not understood. Interestingly, for some nucleotide sugars, like for example UDP-GalNAc, which was shown to accumulate in plant tissues (9), no

target molecule carrying the corresponding sugar moiety has been identified. Hence, the cellular function of several nucleotide sugars is completely unknown in plants (1).

Protein glycosylation can have an influence on protein folding and stability, interaction with proteins and ligands, or enzymatic activity (10–12). Protein *N*-glycosylation starts within the ER lumen with the transfer of a cytosol-derived core glycan on the nitrogen of an asparagine residue followed by its transformation into a high-mannose glycan (13). After protein transport into the Golgi apparatus, *N*-glycans can be further modified to hybrid, complex or paucimannosidic *N*-glycans. The initial committed step in this process is the addition of a GlcNAc residue to appropriately trimmed glycans by *N*-acetylglucosaminyltransferase I (GnT-I) (14). Whereas there are many examples for luminal protein *O*-glycosylation on serine and threonine residues of mammalian proteins (15), the only luminal *O*-glycosyltransferase described so far in plants adds glycans to hydroxyproline residues of proteins found in the cell wall (16).

Glycosylation is essential for protein folding and maturation in the ER, which is equipped with a quality control (ERQC) system that safeguards correct folding and assembly of secretory and membrane proteins in eukaryotic cells and that eliminates improperly folded proteins (17). Under stress conditions, misfolded

## Significance

Nucleotide sugars are donor substrates for the formation of glycan modifications, which are important for the function of many macromolecules such as proteins and lipids. Although most of the glycosylation reactions occur in the endoplasmic reticulum (ER) and Golgi of eukaryotic cells, nucleotide sugar activation occurs in the cytosol and specific transporters must carry these molecules across the membrane. We identified REPRESSOR OF CYTOKININ DEFICIENCY 1 (ROCK1) as an ER-localized transporter of UDP-GlcNAc and UDP-GalNAc in plants. In contrast to animals, nothing is known about the function of the two respective sugar residues in the plant ER. We demonstrate that ROCK1-mediated transport plays a role in the ER-associated protein quality control and loss of *ROCK1* enhances cytokinin responses by suppressing the activity of cytokinin-degrading CKX proteins.

Author contributions: M.C.E.N., I.B., T.S., and T.W. designed research; M.C.E.N., I.B., A.A., H.W., O.N., L.S., and R.S. performed research; M.C.E.N., I.B., A.A., H.W., O.N., L.S., M.S., R.S., H.B., T.S., and T.W. analyzed data; and M.C.E.N. and T.W. wrote the paper.

The authors declare no conflict of interest.

This article is a PNAS Direct Submission.

<sup>1</sup>To whom correspondence should be addressed. Email: tower@zedat.fu-berlin.de.

This article contains supporting information online at [www.pnas.org/lookup/suppl/doi:10.1073/pnas.1419050112/-DCSupplemental](http://www.pnas.org/lookup/suppl/doi:10.1073/pnas.1419050112/-DCSupplemental).

proteins can accumulate in the ER, which leads to ER stress. This triggers an unfolded protein response (UPR) that alleviates ER stress through enhanced expression of genes encoding components of the protein folding machinery or the ER-associated degradation (ERAD) system (18).

Growth and development of plants is controlled by phytohormones. Among them, a group of  $N^6$ -substituted adenine derivatives called cytokinins (CKs) play an important role in many developmental processes, like regulation of cell proliferation and differentiation in root and shoot apical meristems (SAM) (19–21). The catabolic degradation of CKs is mediated by CK oxidase/dehydrogenase (CKX) enzymes encoded by seven genes in *Arabidopsis* (22) and their overexpression causes a CK deficiency characterized by complex morphological changes such as a smaller SAM, a dwarfed shoot, and enhanced root growth (19). *ckx3,5* *Arabidopsis* plants develop more active generative shoot meristems, larger flower organs, and more ovules (23). This demonstrates an important role of regulated CK degradation in defining the CK status of a given tissue. Most CKXs are probably *N*-glycoproteins (22, 24) and the role of glycosylation in fine tuning CKX activity has been discussed (25); however, the hypothesis has not been confirmed and no direct analysis of in planta glycosylation of individual CKX proteins has been reported.

Here we describe a suppressor allele of CK deficiency named *repressor of cytokinin deficiency 1* (*rock1*). Transport assays revealed *ROCK1* to be the first transporter of UDP-GlcNAc and UDP-GalNAc identified in plants. We present data demonstrating that *ROCK1* plays an important role in regulating CK responses and activity of the generative SAM through modulating the activity of CKX proteins. We provide evidence suggesting that the activity of *ROCK1*, in supplying the substrate(s) for a yet to be described protein modification, is important for ERQC in plants.

## Results

***rock1* Decreases the CKX Activity.** To identify new molecular components required for the proper activity of the CK system, we carried out a genetic screen for suppressor alleles of the CK deficiency syndrome displayed by *35S:CKX1* plants. The isolated mutant line *rock1* was characterized by restored rosette size, leaf and flower number, flowering time and, to a lesser extent, root growth (Fig. 1A and *SI Appendix*, Fig. S1). Genetic analysis showed that *rock1-1* is a recessive second-site allele (*SI Appendix*, Table S1) not affecting *35S:CKX1* transgene expression (*SI Appendix*, Fig. S1C).

To understand whether *rock1* directly influenced the CK status, the transcript levels of primary CK response genes, A-type *Arabidopsis* response regulators (*ARRs*), were analyzed in the suppressor line. The mRNA levels of all analyzed *ARR* genes were restored almost to those found in wild type (Fig. 1B). Next, we analyzed the impact of *rock1* mutation on the endogenous CK content. Because *rock1-1* had stronger effects on shoot than on root development, we determined the CK content specifically in seedling shoots and inflorescences of the suppressor line. CK levels in the *rock1-1* suppressor line were five- and twofold increased in comparison with shoots and inflorescences of the parental *35S:CKX1* line, respectively (*SI Appendix*, Tables S2 and S3); however, the restoration of the CK content was not complete.

To gain information about the specificity of *rock1* in suppressing *CKX* overexpression phenotypes, *rock1-1* was introgressed into *35S:CKX2*, *35S:CKX3* (19) and *35S:CKX7* plants (26). Whereas *rock1-1* fully suppressed phenotypes caused by overexpression of *CKX2* and *CKX3* proteins localizing to the secretory pathway (Fig. 1C), it had no effect on the phenotypes caused by the overexpression of the cytosolic *CKX7* isoform (*SI Appendix*, Fig. S1D). Further genetic analysis revealed that *rock1* had only weak or no effect in suppressing shoot phenotypes of mutant plants lacking two or all three CK receptors (27), respectively (*SI Appendix*, Fig. S1). Similarly, the phenotype of

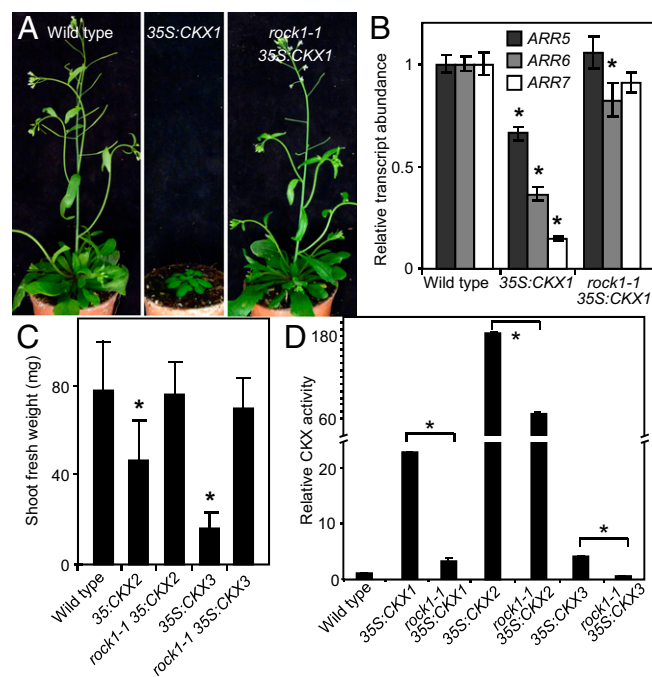


**Fig. 1.** *rock1* suppresses the cytokinin deficiency phenotype by repressing CKX activity. (A) Suppression of the *35S:CKX1* shoot phenotype by *rock1-1* mutation in 4-wk-old plants. (B) Relative transcript abundance of A-type *ARR* genes in shoots of soil-grown seedlings 10 d after germination (dag) measured by quantitative real-time PCR. Data are means  $\pm$  SD ( $n = 4$ ; \* $P < 0.05$ ,  $t$  test). (C) Effect of *rock1-1* on shoot development in plants expressing *35S:CKX2* or *35S:CKX3*. The shoot fresh weight of soil-grown plants was determined 17 dag (means  $\pm$  SD,  $n \geq 15$ ). Significant differences to wild type were determined by  $t$  test (\* $P < 0.05$ ). (D) CKX activity measured in total protein extracts. Activity is expressed relative to wild type. Values are means  $\pm$  SD ( $n \geq 3$ ). Significant differences to the respective CKX overexpression line were determined by  $t$  test (\* $P < 0.05$ ).

mutants lacking multiple CK biosynthetic isopentenyltransferase (*IPT*) genes (28) was only partially suppressed by *rock1-1* (*SI Appendix*, Fig. S1G). Interestingly, comparable restoration of *ipt3,5,7* growth was induced by the application of a chemical inhibitor of CKX activity (29) (*SI Appendix*, Fig. S1G).

Together, the extensive genetic analysis indicated that the main molecular targets of *rock1* in suppressing CK deficiency are CKX proteins associated with the secretory pathway. To test this hypothesis biochemically, the CKX activity in *35S:CKX1* parental line and *rock1* suppressor was compared. Whereas the CKX activity in *35S:CKX1* seedlings was 22-fold higher in comparison with wild type, *rock1* reduced the activity to a level only threefold higher than that of wild type (Fig. 1D). Likewise, the enhanced CKX activity in *35S:CKX2* and *35S:CKX3* plants was reduced through *rock1* introgression by 64% and 100%, respectively (Fig. 1D), supporting the notion of *rock1* affecting CKX proteins.

### ***ROCK1* Encodes an NST Transporting UDP-GlcNAc and UDP-GalNAc.**

The *rock1-1* mutation was mapped to a 49-kb interval on chromosome 5. Sequencing candidate genes revealed a G-to-A transition in the first exon of the *At5g65000* gene leading to a Gly-to-Arg substitution at amino acid position 29 (*SI Appendix*, Fig. S2). This substitution is in the first predicted transmembrane domain of the previously uncharacterized protein of the NST family (*SI Appendix*, Fig. S2). A mutation, *thin-exine2* (*tex2*), in the *At5g65000* gene was previously linked to defective pollen exine production (30). Introduction of a genomic complementation construct into *rock1-1 35S:CKX1* plants resulted in a full recapitulation of *35S:CKX1* phenotypes, confirming that the

*rock1-1* mutation was causative for the suppression phenotype (SI Appendix, Fig. S2D). This was further corroborated by isolating two T-DNA insertion null alleles, *rock1-2* (30) and *rock1-3* (SI Appendix, Fig. S2), which displayed similar developmental changes as *rock1-1* (see below).

To identify the subcellular compartment in which ROCK1 functions, we transiently expressed ROCK1 N- and C-terminally fused to GFP under control of the 35S promoter in *Nicotiana benthamiana* and studied the cellular distribution of the fluorescence signal. The expression of GFP-ROCK1 led to a reticulate GFP signal that colocalized with an ER, but not Golgi, marker (Fig. 2A and SI Appendix, Fig. S3A). In contrast, the ROCK1-GFP fusion clearly colocalized with the Golgi marker (SI Appendix, Fig. S3A), suggesting the possible presence of a C-terminal ER retention/retrieval signal. Indeed, after deleting six C-terminal amino acids in GFP-ROCK1 (GFP-ROCK1<sup>1-319</sup>) containing a cluster of five Lys residues, the GFP signal localized mainly in motile dots colocalizing with a Golgi marker and only a very weak ER signal was observed (Fig. 2A). To rule out the possibility that the N-terminal GFP fusion masked an important localization signal, ROCK1 was internally fused with GFP

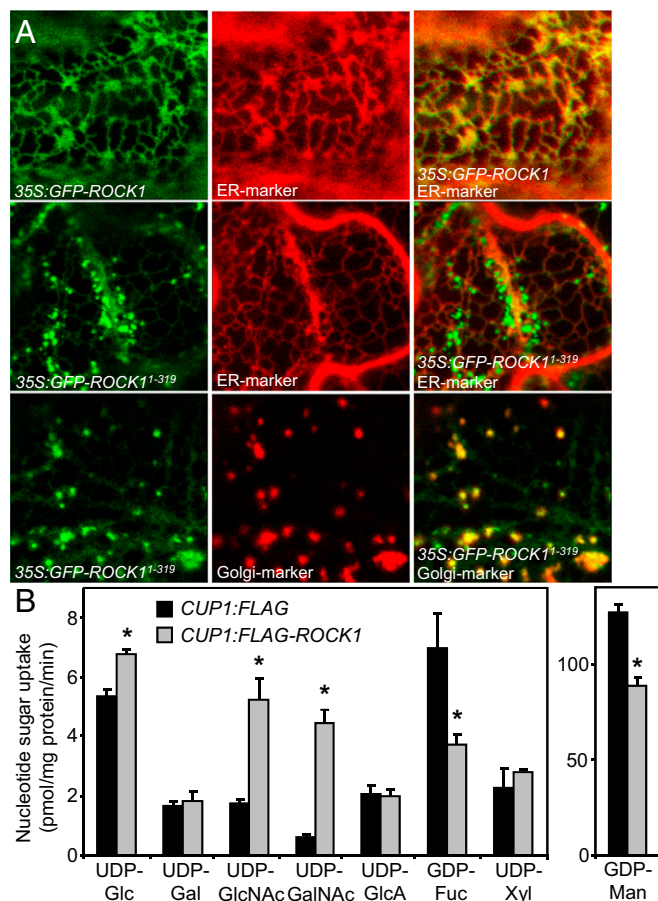


**Fig. 2.** ROCK1 encodes an ER-localized nucleotide sugar transporter. (A) Subcellular localization of ROCK1. 35S:GFP-ROCK1 (Upper) and 35S:GFP-ROCK1<sup>1-319</sup> lacking the putative di-lysine signal (Middle and Lower) were transiently expressed in *N. benthamiana* leaves and colocalization with marker proteins for ER and Golgi (red) were analyzed. (B) Measurement of ROCK1-mediated uptake of radiolabeled nucleotide sugars into yeast microsomes expressing FLAG-ROCK1 or empty vector. Means  $\pm$  SEM ( $n = 3$ ; \* $P < 0.05$ ,  $t$  test). Fuc, fucose; Gal, galactose; GalNAc, *N*-acetylgalactosamine; Glc, glucose; GlcNAc, *N*-acetylglucosamine; GlcA, glucuronic acid; Man, mannose; UDP, uridine diphosphate; Xyl, xylose.

(ROCK1-GFPin) and expressed stably under the *ROCK1* promoter in *rock1-1* plants. A characteristic net-like GFP signal was detected, indicating that the fusion protein localized to the ER (SI Appendix, Fig. S3B). Again, a C-terminal truncation (ROCK1:ROCK1<sup>1-319</sup>-GFPin) relocated the GFP signal into the Golgi (SI Appendix, Fig. S3C) and only a weak ER signal was detected. Interestingly, both constructs were able to fully complement *rock1-1* 35S:CKX1 plants (SI Appendix, Fig. S3D). Together, these results revealed that ROCK1 is an ER-resident protein whose localization is largely controlled by its C-terminal di-lysine motif (31).

The molecular function of ROCK1 has so far not been directly studied. Sequence analysis showed that the closest homologs in *Arabidopsis* are two proteins with unknown function, AT2G43240 and AT4G35335, and CMP-sialic acid transporter AT5G41760 (6) (SI Appendix, Fig. S4) with only low,  $\sim 15\%$ , sequence identity to ROCK1, suggesting that the substrate cannot be inferred from the sequence comparison and, also, that no functional paralogs may exist in *Arabidopsis*. Consistently, usually a single orthologous sequence was identified in other sequenced plant species. To directly test the transport specificity of ROCK1, a FLAG-tagged ROCK1 protein was expressed in *Saccharomyces cerevisiae*, which has, with the exception of GDP-Man, a low background for most nucleotide sugar transport activities and is commonly used as a heterologous test system for NSTs (32). ER/Golgi microsomal vesicles isolated from ROCK1 and empty vector control transformed cells were tested in vitro for transport activity with a range of commercially available radiolabeled nucleotide sugars (Fig. 2B). In vesicles expressing ROCK1 the uptake of UDP-GalNAc and UDP-GlcNAc was seven- and threefold increased, respectively, in comparison with the control (Fig. 2B). A low but significant increase was also detected for UDP-Glc. Interestingly, the relative transport of GDP-Man and GDP-Fuc, which is also mediated by the intrinsic yeast GDP-Man transporter (33), was lowered in the ROCK1 microsomes for unknown reasons. Taken together, these data clearly show that ROCK1 functions as a NST transporting UDP-GalNAc and UDP-GlcNAc as main substrates.

**ROCK1 Regulates the Activity of the Shoot Apical Meristem.** To understand the function of *ROCK1* under physiological conditions, we analyzed the *rock1* mutations in the absence of the 35S:CKX1 transgene. The most prominent morphological changes were observed during generative growth, which was overall accelerated in *rock1* plants. All three *rock1* mutants developed enlarged inflorescences (Fig. 3A) and detailed analysis showed that the frequency of flower initiation was increased by 30% in comparison with wild type. Additionally, stem elongation was accelerated by up to 23% (Fig. 3B). Seven weeks after germination, *rock1* had generated  $\sim 50\%$  more flowers and siliques on the main stem than did the wild type (Fig. 3B). Continuous flower initiation results from the activity of the inflorescence meristem (IM). Scanning electron microscopy analysis revealed that the IM in *rock1* was strongly enlarged and initiated supernumerary flower primordia (Fig. 3C), demonstrating that the enhanced flower formation in *rock1* plants was due to increased IM activity and that *ROCK1* plays a negative regulatory role in this process. These phenotypic changes were strongly reminiscent of those caused by the loss of the *CKX3* and *CKX5* genes (23).

Transcript levels of A-type *ARR* genes were elevated in *rock1* shoots (SI Appendix, Fig. S5A) and the activity of the CK reporter *ARR5:GUS* was increased in the shoot meristem of *rock1* plants (Fig. 3D), suggesting that *ROCK1* regulates SAM activity through adjusting CK signaling in the meristem. Endogenous CK levels were increased up to 35% in *rock1* inflorescences in comparison with the control (SI Appendix, Tables S4 and S5). In accordance with the observed changes in meristem development, the *ROCK1:ROCK1-GUS* reporter construct revealed that *ROCK1* is strongly expressed in the SAM and young flowers (Fig. 3E), supporting

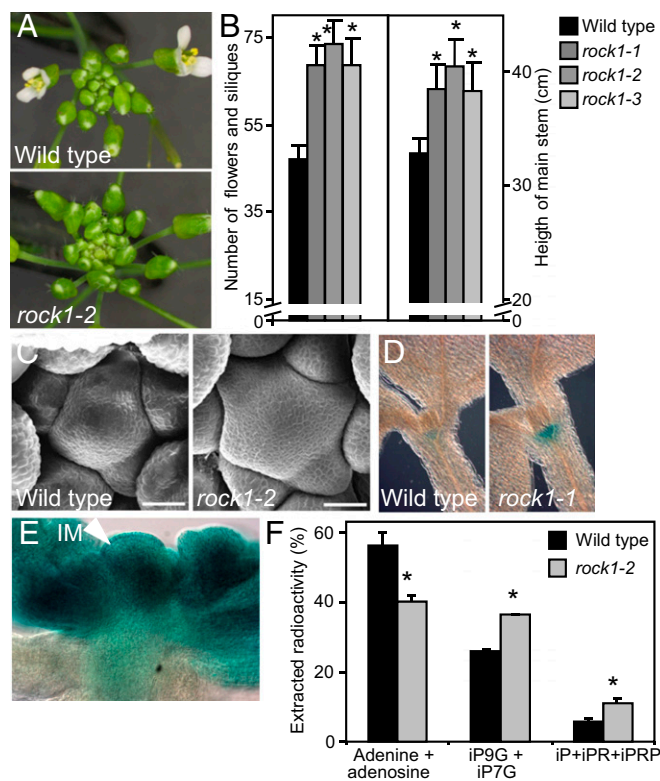


**Fig. 3.** *ROCK1* regulates the activity of the shoot apical meristem. (A) The main inflorescence of the wild-type and *rock1-2* plants 5 wk after germination. (B) Number of flowers and siliques (stages 13–18) and height of the main stem of 7-wk-old *rock1* mutants and wild type. Values are means  $\pm$  SD ( $n \geq 20$ ;  $*P < 0.05$ ,  $t$  test). (C) Scanning electron micrographs of inflorescence meristems (IM) of 4-wk-old wild-type and *rock1-2* plants. (Scale bar, 30  $\mu$ m). (D) Activity of the cytokinin reporter construct *ARR5:GUS* in the shoot meristems of *Arabidopsis* seedlings 2 dag. Staining performed for 1 h. (E) Histochemical detection of *ROCK1:ROCK1-GUS* activity in the IM and young flowers. (F) Analysis of cytokinin metabolite profiles in wild-type and *rock1* seedlings after feeding with  $^3\text{H}$ [iP] for 2 h. Values are means  $\pm$  SD ( $n = 3$ ;  $*P < 0.05$ ,  $t$  test). iP9G/iP7G, iP-N9/7-glucoside; iPR, iP riboside; iPRP, iPR 5'-phosphate.

a direct role of *ROCK1* in regulating shoot meristem development. The reporter construct further revealed expression of *ROCK1* in numerous other tissues (SI Appendix, Fig. S6); however, we observed neither changes in root development nor altered responses to exogenous CK in *rock1* roots (SI Appendix, Fig. S5), supporting the notion that *ROCK1* is more relevant for regulating CK responses in the shoot.

To analyze whether *rock1* alters CK responses through regulating CKX activity also under physiological conditions, we performed feeding experiments in which we supplied plants with radiolabeled CK (isopentenyladenine, iP) and followed its metabolic conversion. The level of degradation products of CKX reaction was reduced by 30% in *rock1* plants after a 2-h incubation, whereas the fraction containing iP with the corresponding riboside and nucleotide was significantly larger in comparison with wild type (Fig. 3F). This further substantiates a *ROCK1* regulatory function in tuning CKX-mediated CK degradation.

***ROCK1* Plays an Important Role in ERQC.** Next we aimed to analyze the molecular mechanism underlying the regulation of CKX activity and to understand the function of *ROCK1*-transported substrates in this process. Whereas there is virtually no cellular activity requiring UDP-GalNAc known in plants, UDP-GlcNAc is a substrate of GnT-I in a step converting high mannose to hybrid and complex *N*-glycans. We tested CKX1 glycosylation

and the nature of linked *N*-glycans. Total proteins from *Arabidopsis* plants expressing N-terminally myc-tagged CKX1 (myc-CKX1) from the 35S promoter were extracted and subjected to treatment with peptide *N*-glycosidase F (PNGase F) removing all *N*-linked oligosaccharides except those carrying core  $\alpha$ 1,3-fucose. Immunoblot analysis revealed an electrophoretic mobility shift of myc-CKX1 (Fig. 4A), showing that the protein contains *N*-linked oligosaccharides. Treatment with endoglycosidase H (EndoH), which is unable to cleave complex *N*-glycans, resulted in a similar mobility shift of myc-CKX1, suggesting that CKX1 contains mainly high-mannose *N*-glycans. Interestingly, *ROCK1* is not substantially involved in CKX1 *N*-glycosylation as myc-CKX1 extracted from *rock1-1* plants showed no obvious difference in mass compared with myc-CKX1 from wild type and was comparably affected by PNGase F and EndoH treatment (Fig. 4A). Similarly, *rock1* did not influence the overall protein modification with complex *N*-glycans as indicated by the immunoblot analysis with antibodies against complex *N*-glycans (SI Appendix, Fig. S7).

To test unequivocally whether CKX1 activity is dependent on hybrid or complex *N*-glycans, the *complex glycans less 1* (*cgl1*) mutation of GnT-I was introgressed into 35S:CKX1 plants. As Fig. 4B shows, *cgl1-2* had no effect on the 35S:CKX1 phenotype, indicating that CKX1 function is independent of GnT-I activity and further supporting the idea that *ROCK1* does not provide UDP-GlcNAc for this reaction.

The protein immunoblot analysis revealed that the level of myc-CKX1 was consistently lower in *rock1-1* compared with wild type (Fig. 4C), suggesting that CKX1 protein abundance might be controlled by *ROCK1*. To test CKX1 turnover, we analyzed myc-CKX1 levels in the presence of the translation inhibitor cycloheximide (CHX). As shown in Fig. 4D, myc-CKX1 was relatively unstable, with a half-life of  $\sim$ 4 h. The turnover of myc-CKX1 in *rock1* was comparable to wild type (Fig. 4D). Interestingly, treatment with MG132, a widely used inhibitor of the proteasome, increased the level of myc-CKX1 in wild type (Fig. 4E), indicating that CKX1 protein, which has been shown to localize to the ER/secretory system (19), is degraded by a proteasome-dependent ERAD mechanism. Intriguingly, inhibition of the proteasome in the *rock1* background strongly stabilized myc-CKX1 levels (Fig. 4E), suggesting that the lower myc-CKX1 steady-state levels in *rock1* were caused by increased ERAD. Reduced levels of myc-CKX1 could thus indicate inefficient protein processing and folding. This was supported by the analysis of the UPR status through measuring the expression level of typical ER stress response genes, encoding components of the ER protein-folding machinery. Fig. 4F shows that the steady-state transcript levels of the *binding protein 1* (*BiP1*), *calnexin 1* (*CNX1*), and *calreticulin 2* (*CRT2*) genes were significantly increased by up to twofold in *rock1* plants in comparison with wild type, demonstrating that UPR was constitutively enhanced and further suggesting defects in ERQC caused by the *rock1* mutation. To address this notion experimentally, we used a mutant allele of the brassinosteroid receptor gene, *brassinosteroid insensitive 1-9* (*bri1-9*). The gene product is functionally competent as a hormone receptor but is retained by the ERQC system and degraded by ERAD, causing severe dwarfing of this receptor mutant (34) (Fig. 4G). Introgression of *rock1-2* into *bri1-9* led to a strong suppression of the dwarf *bri1-9* phenotype (Fig. 4G), indicating that *bri1-9* leaked from its ER retention machinery, which became compromised in *rock1* in a similar fashion as described for other suppressor genes of *bri1-9* (35). This was confirmed by the detection of an EndoH-resistant, complex *N*-glycan-carrying form of *bri1-9* in *rock1* (SI Appendix, Fig. S9). Hence, our data indicate that *ROCK1* is a very important component of the protein folding machinery and/or ERQC in plants.

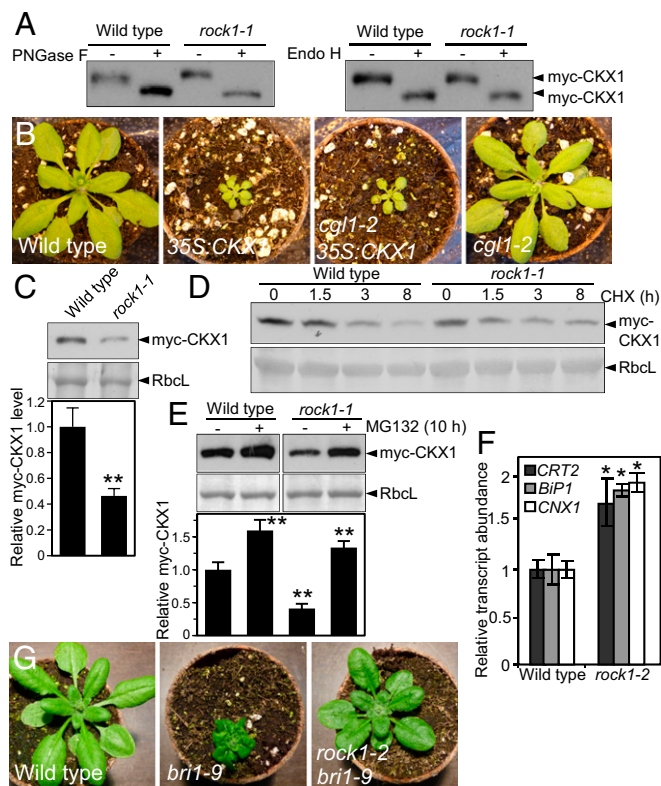


**Fig. 4.** ROCK1 regulates ERQC and CKX protein abundance. (A) *N*-glycosylation status of myc-CKX1 protein in wild-type and *rock1* seedlings. Protein extracts were treated with PNGase F or EndoH and the size of myc-CKX1 was compared with mock-treated control by SDS/PAGE and immunoblot with anti-myc antibody. (B) The loss of GnT-I activity in *cgl1* mutants has no influence on the shoot phenotype of 35S:CKX1 plants (21 dag). (C) The level of myc-CKX1 is decreased in *rock1* compared with wild type. (D) Analysis of myc-CKX1 stability. Total protein extracts were analyzed by immunoblotting with anti-myc antibody. Coomassie blue staining of Rubisco large subunit (RbcL) was used as loading control. Relative densitometric analysis of the myc-CKX1 signal is shown. Values are means  $\pm$  SEM ( $n = 10$ ;  $**P < 0.01$ , *t* test). (E) Analysis of myc-CKX1 stability. Protein extracts were prepared from 7-d-old seedlings treated with mock or 100  $\mu$ M CHX for indicated times and analyzed by immunoblotting. (F) myc-CKX1 is degraded in proteasome-dependent manner. Seedlings were treated with 100  $\mu$ M MG132 and myc-CKX1 analyzed by immunoblotting and densitometry. Means  $\pm$  SEM ( $n = 4$ ;  $**P < 0.01$ , *t* test). (G) Quantitative real-time PCR analysis of UPR genes in shoots of soil-grown seedlings 9 dag. Means  $\pm$  SD are shown ( $n = 4$ ;  $*P < 0.05$ , *t* test). (H) The *rock1* mutation suppresses the brassinosteroid deficiency shoot phenotype of *bri1-9* mutant plants (26 dag).

## Discussion

We could show that *Arabidopsis* ROCK1 is a NST with main transport activity toward UDP-GlcNAc and UDP-GalNAc. Multiple lines of evidence show that ROCK1 is a positive regulator of CKX activity in plants, which raises the question of how transport of these substrates is functionally connected to regulation of CKX proteins.

In the lumen of the plant secretory pathway, UDP-GlcNAc is used for the formation of hybrid or complex *N*-glycans on secreted and membrane proteins (14) and it has been suggested that *N*-glycosylation is relevant for regulating CKX activity (25). Our genetic data showed that CKX1 activity is independent of the presence of complex *N*-glycans, which indicates that the reduced GlcNAc availability for GnT-I in the Golgi was not the cause for the reduced CKX1 activity in *rock1*. In the same line of evidence, the overall protein *N*-glycosylation pattern was not apparently affected in *rock1*, suggesting also that a ROCK1-independent transport route for UDP-GlcNAc into the Golgi

exists. The notion that ROCK1-mediated transport of UDP-GlcNAc does not serve the complex *N*-glycan processing in the Golgi was also supported by localization of ROCK1 in the ER membrane.

Beside the *N*-linked oligosaccharides, various proteins bearing a single GlcNAc residue attached to the Asn of the canonical Asn-X-Ser/Thr sequon have been described in fungi (36) and recently also in animals (37) and plants (38). Interestingly, Kim et al. proposed that such *N*-GlcNAc modifications originate by a mechanism that is, at least in part, different from the cleavage of *N*-linked oligosaccharides (38). The corresponding glycosyltransferase is, however, currently unknown. Additionally, single *O*-linked GlcNAc is a well-studied reversible posttranslational modification of Ser/Thr residues on cytosolic and nuclear proteins of higher eukaryotes (39). Interestingly, an analogous modification has recently been identified on extracellular domains of *Drosophila* Notch protein and the corresponding glycosyltransferase localizes to the ER (40).

ROCK1 was identified to be a multispecific NST with high transport affinity also for UDP-GalNAc. Transport of UDP-GalNAc has recently been described in tobacco (41) and it could be that a ROCK1 homolog is responsible for this activity. However, despite the occurrence and transport of UDP-GalNAc in plants, the function of the corresponding sugar moiety remains obscure. Although plants obviously lack the machinery to produce the, typically mammalian, mucin-type *O*-glycosylation of proteins (41), several earlier reports described GalNAc as part of glycoproteins in higher plants and green algae (42–44). It will be important to investigate whether any of the above discussed rare glycosylations reactions involving GlcNAc or GalNAc occur within the plant ER. A direct comparison of the glycan composition of CKX proteins isolated from wild-type and *rock1* plants could be instrumental in identifying these modifications.

*rock1* was identified due to its capacity to suppress CK deficiency caused by CKX1 overexpression. We could show that CKX1 is an ERAD substrate and that *rock1* mainly affects CKX1 by reducing its abundance. It cannot be currently excluded that *rock1* influences the enzymatic activity and/or subcellular localization of CKX1 as well. This, together with the fact that the myc-CKX1 levels were restored in *rock1* plants upon inhibiting the proteasomal degradation, suggests the protein folding capacity or fidelity is compromised in the *rock1* mutant, resulting in enhanced ERAD of CKX1. The hypothesis, that ROCK1 plays an important role during quality monitoring of secretory proteins in the ER was underpinned by the complete phenotypic suppression of *bri1-9* by *rock1*, which was not an indirect CK effect (*SI Appendix*, Fig. S9). It has been shown previously that, similarly to *rock1*, the loss of other components of the ERQC system leads to leakage of the *bri1-9* protein from the ER and restoration of brassinosteroid responses (35, 45). The exact mechanism of ROCK1 interaction with the ERQC and ERAD pathway is currently unclear. It needs to be investigated whether some of the above discussed glycan modifications serve as a signal for protein folding, quality control, and ERAD. It is also important to keep in mind that for the correct activity of the ERQC machinery an import of UDP-Glc into the ER lumen is required to supply UDP-glucose:glycoprotein glucosyltransferase (UGGT) (17). This enzyme adds glucose to the branched *N*-linked oligosaccharide present in unfolded proteins, to form Glc<sub>1</sub>Man<sub>9</sub>GlcNAc<sub>2</sub>. The terminal glucose present in this structure is bound by chaperones in the calnexin/calreticulin cycle controlling the folding status of glycoproteins in the ER. The loss of UGGT compromises the ERQC in *Arabidopsis*, which leads to *bri1-9* suppression (34). In our assay system, yeast microsomes expressing ROCK1 showed only a weak increment in the transport of UDP-Glc, which could be due to relatively high background transport activity in control microsomes. This raises the question of whether this transport also contributes to the total UDP-Glc influx into the ER in planta and, hence, whether ROCK1 can function, at least partially, in supplying

UDP-Glc for UGGT. This hypothesis is, however, not supported by the work of Reyes et al. (7), who has proposed that AtUTr1 and AtUTr3 are the main, if not the only, NSTs involved in the import of UDP-Glc into the *Arabidopsis* ER. In contrast to these two transporter genes, *ROCK1* expression is not induced by ER stress (SI Appendix, Fig. S10).

The activity of the reproductive SAM was strongly increased in *rock1* to an extent similar to that caused by mutation of *CKX3* and *CKX5* (23). This result is very consistent with the proposed role of *ROCK1* as a positive regulator of CKX proteins, which was further supported by the increased CK content in the *rock1* inflorescences. Thus, the modification of CKX activity by *ROCK1* adds an additional layer of fine tuning of meristem activity and organ formation. It remains to be determined whether *ROCK1* activity modulates CK responses also in other tissues. For example, *ROCK1* was earlier identified in a screen for genes involved in pollen exine development and designated as *THIN-EXINE2* (*TEX2*) (30). The pollen-localized activity of

*ROCK1* reporter shown in this work is consistent with the *tex2* mutant pollen phenotype. It has been shown that CK signaling is involved in regulation of pollen development (46) and it will be interesting to analyze whether CKX isoforms expressed in pollen (19) are regulated by *ROCK1*. Alternatively, it could be that GlcNAc/GalNAc is directly required for the biosynthesis of sporopollenin, which is a major component of the exine layer, or the polysaccharide-containing exine precursor, primumexine (47).

## Materials and Methods

For the plant material, the gene mapping, the cloning of the constructs, the molecular and microscopic analyses, the transport assay, and the cytokinin measurements, see SI Materials and Methods.

**ACKNOWLEDGMENTS.** This work was supported by Deutsche Forschungsgemeinschaft (Schm 814/21 and WE 4325/2), an Elsa-Neumann fellowship (to M.C.E.N.), and Ministry of Education, Youth and Sports of the Czech Republic (LK21306 and LO1204).

- Bar-Peled M, O'Neill MA (2011) Plant nucleotide sugar formation, interconversion, and salvage by sugar recycling. *Annu Rev Plant Biol* 62:127–155.
- Berninsone PM, Hirschberg CB (2000) Nucleotide sugar transporters of the Golgi apparatus. *Curr Opin Struct Biol* 10(5):542–547.
- Rollwitz I, Santaella M, Hille D, Flügge U, Fischer K (2006) Characterization of AtNST-KT1, a novel UDP-galactose transporter from *Arabidopsis thaliana*. *FEBS Lett* 580(17):4246–4251.
- Baldwin TC, Handford MG, Yuseff MI, Orellana A, Dupree P (2001) Identification and characterization of GONST1, a golgi-localized GDP-mannose transporter in *Arabidopsis*. *Plant Cell* 13(10):2283–2295.
- Bakker H, et al. (2005) Molecular cloning of two *Arabidopsis* UDP-galactose transporters by complementation of a deficient Chinese hamster ovary cell line. *Glycobiology* 15(2):193–201.
- Bakker H, et al. (2008) A CMP-sialic acid transporter cloned from *Arabidopsis thaliana*. *Carbohydr Res* 343(12):2148–2152.
- Reyes F, et al. (2010) The nucleotide sugar transporters AtUTr1 and AtUTr3 are required for the incorporation of UDP-glucose into the endoplasmic reticulum, are essential for pollen development and are needed for embryo sac progress in *Arabidopsis thaliana*. *Plant J* 61(3):423–435.
- Mortimer JC, et al. (2013) Abnormal glycosphingolipid mannosylation triggers salicylic acid-mediated responses in *Arabidopsis*. *Plant Cell* 25(5):1881–1894.
- Alonso AP, Piasecki RJ, Wang Y, LaClair RW, Shachar-Hill Y (2010) Quantifying the labeling and the levels of plant cell wall precursors using ion chromatography tandem mass spectrometry. *Plant Physiol* 153(3):915–924.
- Roos MD, Su K, Baker JR, Kudlow JE (1997) O glycosylation of an Sp1-derived peptide blocks known Sp1 protein interactions. *Mol Cell Biol* 17(11):6472–6480.
- Häweker H, et al. (2010) Pattern recognition receptors require N-glycosylation to mediate plant immunity. *J Biol Chem* 285(7):4629–4636.
- Liebming E, Grass J, Altmann F, Mach L, Strasser R (2013) Characterizing the link between glycosylation state and enzymatic activity of the endo- $\beta$ -1,4-glucanase KORRIGAN1 from *Arabidopsis thaliana*. *J Biol Chem* 288(31):22270–22280.
- Lerouxel O, et al. (2005) Mutants in DEFECTIVE GLYCOSYLATION, an Arabidopsis homolog of an oligosaccharyltransferase complex subunit, show protein underglycosylation and defects in cell differentiation and growth. *Plant J* 42(4):455–468.
- von Schaewen A, Sturm A, O'Neill J, Chrispeels MJ (1993) Isolation of a mutant *Arabidopsis* plant that lacks N-acetylglucosaminyl transferase I and is unable to synthesize Golgi-modified complex N-linked glycans. *Plant Physiol* 102(4):1109–1118.
- Bennett EP, et al. (2012) Control of mucin-type O-glycosylation: A classification of the polypeptide GalNAc-transferase gene family. *Glycobiology* 22(6):736–756.
- Velasquez SM, et al. (2011) O-glycosylated cell wall proteins are essential in root hair growth. *Science* 332(6036):1401–1403.
- Ellgaard L, Helenius A (2003) Quality control in the endoplasmic reticulum. *Nat Rev Mol Cell Biol* 4(3):181–191.
- Römisch K (2005) Endoplasmic reticulum-associated degradation. *Annu Rev Cell Dev Biol* 21:435–456.
- Werner T, et al. (2003) Cytokinin-deficient transgenic *Arabidopsis* plants show multiple developmental alterations indicating opposite functions of cytokinins in the regulation of shoot and root meristem activity. *Plant Cell* 15(11):2532–2550.
- Dello Iorio R, Linhares FS, Sabatini S (2008) Emerging role of cytokinin as a regulator of cellular differentiation. *Curr Opin Plant Biol* 11(1):23–27.
- Gordon SP, Chickarmane VS, Ohno C, Meyerowitz EM (2009) Multiple feedback loops through cytokinin signaling control stem cell number within the *Arabidopsis* shoot meristem. *Proc Natl Acad Sci USA* 106(38):16529–16534.
- Schmülling T, Werner T, Riefler M, Krupková E, Bartrina y Manns I (2003) Structure and function of cytokinin oxidase/dehydrogenase genes of maize, rice, *Arabidopsis* and other species. *J Plant Res* 116(3):241–252.
- Bartrina I, Otto E, Strnad M, Werner T, Schmülling T (2011) Cytokinin regulates the activity of reproductive meristems, flower organ size, ovule formation, and thus seed yield in *Arabidopsis thaliana*. *Plant Cell* 23(1):69–80.
- Morris RO, Bilyeu KD, Laskey JG, Cheikh NN (1999) Isolation of a gene encoding a glycosylated cytokinin oxidase from maize. *Biochem Biophys Res Commun* 255(2):328–333.
- Motyka V, et al. (2003) Cytokinin-induced upregulation of cytokinin oxidase activity in tobacco includes changes in enzyme glycosylation and secretion. *Physiol Plant* 117:11–21.
- Köllmer I, Novák O, Strnad M, Schmülling T, Werner T (2014) Overexpression of the cytosolic cytokinin oxidase/dehydrogenase (CKX7) from *Arabidopsis* causes specific changes in root growth and xylem differentiation. *Plant J* 78(3):359–371.
- Riefler M, Novák O, Strnad M, Schmülling T (2006) *Arabidopsis* cytokinin receptor mutants reveal functions in shoot growth, leaf senescence, seed size, germination, root development, and cytokinin metabolism. *Plant Cell* 18(1):40–54.
- Miyawaki K, et al. (2006) Roles of *Arabidopsis* ATP/ADP isopentenyltransferases and tRNA isopentenyltransferases in cytokinin biosynthesis. *Proc Natl Acad Sci USA* 103(44):16598–16603.
- Zatloukal M, et al. (2008) Novel potent inhibitors of *A. thaliana* cytokinin oxidase/dehydrogenase. *Bioorg Med Chem* 16(20):9268–9275.
- Dobritsa AA, et al. (2011) A large-scale genetic screen in *Arabidopsis* to identify genes involved in pollen exine production. *Plant Physiol* 157(2):947–970.
- Benghezal M, Wasteneys GO, Jones DA (2000) The C-terminal dilysine motif confers endoplasmic reticulum localization to type I membrane proteins in plants. *Plant Cell* 12(7):1179–1201.
- Gerardy-Schahn R, Oelmann S, Bakker H (2001) Nucleotide sugar transporters: Biochemical and functional aspects. *Biochimie* 83(8):775–782.
- Ashikov A, et al. (2005) The human solute carrier gene SLC35B4 encodes a bifunctional nucleotide sugar transporter with specificity for UDP-xylose and UDP-N-acetylglucosamine. *J Biol Chem* 280(29):27230–27235.
- Jin H, Yan Z, Nam KH, Li J (2007) Allele-specific suppression of a defective brassinosteroid receptor reveals a physiological role of UGGT in ER quality control. *Mol Cell* 26(6):821–830.
- Hong Z, et al. (2009) Mutations of an alpha1,6 mannosyltransferase inhibit endoplasmic reticulum-associated degradation of defective brassinosteroid receptors in *Arabidopsis*. *Plant Cell* 21(12):3792–3802.
- Hase S, Fujimura K, Kanoh M, Ikenaka T (1982) Studies on heterogeneity of Takamylase A: Isolation of an amylase having one N-acetylglucosamine residue as the sugar chain. *J Biochem* 92(1):265–270.
- Chalkley RJ, Thalhammer A, Schoepfer R, Burlingame AL (2009) Identification of protein O-GlcNAcylation sites using electron transfer dissociation mass spectrometry on native peptides. *Proc Natl Acad Sci USA* 106(22):8894–8899.
- Kim YC, et al. (2013) Identification and origin of N-linked  $\beta$ -D-N-acetylglucosamine monosaccharide modifications on *Arabidopsis* proteins. *Plant Physiol* 161(1):455–464.
- Hart GW, Housley MP, Slawson C (2007) Cycling of O-linked beta-N-acetylglucosamine on nucleocytoplasmic proteins. *Nature* 446(7139):1017–1022.
- Sakaidani Y, et al. (2011) O-linked-N-acetylglucosamine on extracellular protein domains mediates epithelial cell-matrix interactions. *Nat Commun* 2:583.
- Yang Z, et al. (2012) Toward stable genetic engineering of human O-glycosylation in plants. *Plant Physiol* 160(1):450–463.
- Hori H (1978) The demonstration of galactosamine in extracellular hydroxyproline-rich macromolecule purified from the culture media of tobacco cells. *Plant Cell Physiol* 19(3):501–505.
- Lenucci M, Leucci MR, Andreoli C, Dalessandro G, Piro G (2006) Biosynthesis and characterization of glycoproteins in *Koeleria antarctica* (Klebsormiales, Chlorophyta). *Eur J Phycol* 41(2):213–222.
- Wold JK, Hillestad A (1976) The demonstration of galactosamine in a higher plant: *Cannabis sativa*. *Phytochemistry* 15(2):325–326.
- Jin H, Hong Z, Su W, Li J (2009) A plant-specific calcitriculin is a key retention factor for a defective brassinosteroid receptor in the endoplasmic reticulum. *Proc Natl Acad Sci USA* 106(32):13612–13617.
- Kinoshita-Tsujiyama K, Kakimoto T (2011) Cytokinin receptors in sporophytes are essential for male and female functions in *Arabidopsis thaliana*. *Plant Signal Behav* 6(1):66–71.
- Ariizumi T, Toriyama K (2011) Genetic regulation of sporopollenin synthesis and pollen exine development. *Annu Rev Plant Biol* 62:437–460.

## SI Appendix

### SI Materials and Methods

#### Plant material, growth conditions, genotyping and plant transformation

If not otherwise denoted, *Arabidopsis thaliana* Columbia-0 was used as the wild type. The T-DNA insertion lines *rock1-2* (SALK\_001259) and *rock1-3* (901C01) were used. The following lines were described previously: 35S:CKX1-11, 35S:CKX2-9, 35S:CKX3-9 (1), 35S:CKX7-GFP-26 (2), *ahk2-5*, *ahk3-7*, *cre1-2* (3), *atipt1*, *atipt3-2*, *atipt5-2*, *atipt7-1* (4), *cgl1 C6* (*cgl1-2*) (5) and *ARR5:GUS* (6). Mutant lines were genotyped by PCR and dCAPS analysis using primers listed in Table S6 and S7, respectively.

Plants were grown in vitro on half-strength Murashige and Skoog (MS) medium containing 10 g/L sucrose, 0.5 g/L MES and 8 g/L phytigel. For analysis of root growth, 12 g/L phytigel and cytokinin or DMSO as solvent control were added to the medium. Plants were grown under long day conditions (16h light / 8h dark; 21 / 18°C) in vitro or in the green house. Shoots of soil grown plants were sprayed with 10 µM INCYDE (7) and 0.01% Silwet L-77 every 3 days starting 3 days after germination.

The binary vector constructs were transformed into *Arabidopsis* plants by *Agrobacterium tumefaciens* (strain GV3101:pMP90) mediated floral dip method (8).

#### EMS mutagenesis and mapping

35S:CKX1 seeds were incubated with 0.2% ethyl methanesulfonate for 16 h and progeny of 1,100 M1 individuals were analyzed. By analyzing 1164 F2 recombinants from the cross between *rock1-1* 35S:CKX1 and *Arabidopsis Landsberg erecta*, *rock1-1* was mapped to a 49-kb region (~0.13 cM) on the BAC clone MXK3. *rock1-1* mutation was identified by sequencing candidate genes.

#### DNA cloning

All primers used are listed in table S9. The *ROCK1:ROCK1* construct used for complementation was prepared by amplifying a 4.3 kb large genomic fragment using primer 1 and 2. The fragment was cloned into the *SacI* site of pCB302 (9).

*ROCK1:ROCK1-GUS* was cloned by amplifying a genomic fragment including a 1.8 kb promoter region of *ROCK1* and the whole coding region without the stop codon using primer 3 and 4. The amplicon was digested with *NdeI* and ligated into the *XbaI* site of the vector pCB308 (9).

For obtaining the construct *CUP1:FLAG-ROCK1*, the *ROCK1* cDNA was amplified with the primer 5 and 6 using the SALK clone U87105 as template and cloned into the *KpnI* and *EcoRI* sites of pYEScupFLAGK (10).

To generate the construct 35S:*myc-CKX1*, the *CKX1* cDNA was PCR-amplified in two steps by using primer pairs 7/8 and 9/10. The final amplicon was cloned into the vector pDONR221 (Invitrogen) and subsequently pGWB18 (11).

To create 35S:*GFP-ROCK1*, the *ROCK1* genomic coding sequence was PCR-amplified in two steps by using primer pairs 11/12 and 9/10 and cloned into pDONR222 (Invitrogen) and subsequently into pK7WGF2 (12). The primer pair 11/13 was used for cloning the truncated *ROCK1* version in the 35S:*GFP-ROCK1*<sup>1-319</sup> construct. To create 35S:*ROCK1-GFP*, the *ROCK1* genomic coding sequence was PCR-amplified by using primer pairs 11/14 and 9/10 and cloned into pDONR222 and

subsequently into pB7FWG2 (12). To create *ROCK1:ROCK1-GFPin*, the sequence encoding *eGFP* was amplified with primer 15 and 16 using the vector pB7FWG2 as template and cloned into the *VspI* site of the vector pCB302-ROCK1:ROCK1 described above. To create *ROCK1:ROCK1<sup>1-319</sup>-GFPin*, the GFP and the 0.4 kb *EcoRI* fragment were deleted from the vector pCB302-ROCK1:ROCK1-GFPin by partial digestion with *VspI* and *EcoRI* creating part 1. A fusion construct consisting of GFP and the *ROCK1* 3' part was PCR-amplified using the primer 15 and 17 and pCB302-ROCK1:ROCK1-GFPin as template, further digested by *VspI* and partially digested by *EcoRI*. The resulting 0.7 kb fragment was ligated with part 1 and GFP inserted into the *VspI* site. All cloned sequences were verified by sequencing.

### **RNA extraction, cDNA synthesis and qPCR**

Whole RNA was extracted from tissues by TRIzol method (13). Samples were treated with DNase I (Thermo Scientific) and 2 µg RNA were transcribed into cDNA by Superscript III reverse transcriptase (Invitrogen) using a 25-mer oligo-dT primer at 2.5 µM and a 9-mer random primer at 4.5 µM. 50 ng cDNA were used as template in a qPCR reaction consisting of 0.01 U/µL Immolase DNA-Polymerase (BioLine), the corresponding 1x buffer, 2 mM MgCl<sub>2</sub>, 100 µM each dNTP, 0.1x SYBR Green I (Fluka), 50 nM ROX (Sigma) and 300 nM each primer (Table S8) in a final volume of 20 µL. qPCR analysis was done using a 7500 Fast Real-Time PCR system (Applied Biosystems). The qPCR temperature program consisted of the following steps: 95°C for 15 min; 40 cycles of 95°C 15 s, 55°C 15 s, 72°C 15 s; followed by melting curve analysis. Relative transcript abundance of each gene was calculated based on the  $\Delta\Delta C_t$  method (14). *β-Tubulin* or *UBC10* were used for normalization.

### **CKX activity assay**

CKX activity in seedling extracts was determined by a modified end-point method (15). Seedlings were frozen in liquid nitrogen and grinded in a tissue-mill (Retsch) to a fine powder. 1.5 to 2 mL extraction buffer (0.2 M Tris-HCl pH 7.5, 0.3% Triton X-100, complete protease inhibitor cocktail without EDTA (Roche)) was added per 1 g of plant material and incubated for 20 min on ice followed by centrifugation at 2,000g for 5 min. The protein concentrations in the supernatants were measured using a bicinchoninic acid protein assay kit (Pierce). 200 µL (35S:CKX1 and 35S:CKX3 plants) or 50 µL (35S:CKX2 plants) of the extract were incubated with 500 µL ferricyanide (CKX1 and CKX3) or 2,6-dichlorophenol indophenol (CKX2), 100 mM McIlvaine buffer (CKX1 and CKX3 pH 5, CKX2 pH 6.5) and 250 µM iP9G (CKX1) or iP (CKX2 and CKX3) in a final volume of 600 µL. The reaction was incubated for 1-2 h at 37°C, stopped by 0.3 mL 40% trichloroacetic acid (TCA) and centrifuged at 16,000g for 5 min. 850 µL of the supernatant were mixed with 200 µL 2% 4-aminophenol (dissolved in 6% TCA), incubated for 1 min and the concentration of the formed Schiff base determined by measuring the absorption at 352 nm.

### **Transient expression in *N. benthamiana* and confocal laser scanning microscopy**

Infiltration was performed as described previously (16) using *A. tumefaciens* strain GV3101:pMP90 and 6-week-old *N. benthamiana* plants. For co-expression, the *Agrobacterium* cultures harbouring different expression constructs were mixed in infiltration medium to a final OD<sub>600</sub> of 0.05 for each.

35S:p19 (17) was included in all infiltrations. GFP-fusion proteins and mCherry-marker proteins, CD3-959 and CD3-967 (18), were analyzed by confocal laser scanning microscope (TCS SP5, Leica) 3-5 days after infiltration. GFP and mCherry were excited at 488 nm and 561 nm and the fluorescence detected at 498-538 nm and 600-630 nm, respectively.

### **Deglycosylation assays and immunoblot analysis**

For myc-CKX1 analysis, proteins were extracted and the concentration determined as described for the CKX activity assay. Proteins were separated by 10% SDS-PAGE and blotted on PVDF membrane (Millipore). Membranes were blocked with 5% skim milk in PBS containing 0.1% Tween 20. A mouse monoclonal anti-myc antibody (clone 4A6, Millipore, dilution 1:2500) followed by a goat anti-mouse antibody coupled to horse radish peroxidase (sc-2005, Santa-Cruz, dilution 1:5000) was used to detect myc-CKX1. Bound antibodies were visualized with SuperSignal West Pico chemiluminescent substrate (Thermo Scientific). Densitometric analysis was performed using the ImageJ software v.1.47 (<http://imagej.nih.gov/ij/>). Intensities were normalized to the loading control and calculated relative to wild type samples. For analysis of the N-glycosylation total proteins were treated by Endoglycosidase H<sub>f</sub> and PNGase F (New England Biolabs) according to the manufacturer prior to SDS-PAGE.

For BRI1 analysis, proteins from 200 mg of 8-d-old seedlings were extracted by dissolving the homogenized plant material in 800 µl RIPA-buffer (Sigma) supplemented with 1% (v/v) protease inhibitor cocktail (Sigma). After centrifugation at 10000 g for 10 min at 4°C, the supernatant was mixed with 3 x SDS sample loading buffer and incubated at 95°C for 5 min. Proteins were separated by SDS-PAGE using a Mini-PROTEAN TGX gradient gel (4%-15%, Bio-Rad), transferred to Hybond ECL membrane (GE Healthcare) and analysed by immunoblotting using BRI1 antibody (Agrisera) diluted 1:5000 in Tris buffered saline (150 mM NaCl, 10 mM Tris-HCl pH 8.0) containing 0.05% Tween 20 and 5% skim milk.

### **GUS staining, microscopy and scanning electron microscopy**

GUS staining was performed as described before (1). For microscopic analysis, tissues were cleared according to Malamy and Benfey (1997) (19). The inflorescence meristem of the main stem from 4 weeks old soil grown plants was dissected and analyzed by scanning electron microscopy as described before (20).

### **Quantification of endogenous cytokinins**

Extraction, purification and quantification by ultraperformance liquid chromatography-electrospray tandem mass spectrometry was performed as described previously (21). At least three independent biological replicates were analyzed for each genotype and tissue.

### **Cytokinin-feeding experiments**

Wild-type and *rock1* seedlings were grown for 8 days in ½ MS liquid medium with 0.1% sucrose. 200 mg seedlings were transferred into medium containing 39 nM <sup>3</sup>H[iP] (32 Ci/mmol, obtained from the Isotope Laboratory of the Institute of Experimental Botany AS CR, Prague, Czech Republic) and incubated for 2 h. Seedlings were washed twice in water and snap-frozen. Cytokinins were extracted

and purified according to protocol described “for set A” in Novák et al. (22), vacuum evaporated at 40°C and resolved in 500 µL 10% methanol. After dephosphorylation, HPLC analyses was performed on an Alliance 2690 Separations Module (Waters, Milford, MA, USA) linked to PDA 996 (Waters, Milford, MA, USA). Samples were separated on a Symmetry C18 column (150 × 2.1 mm, 5 µm, Waters, Milford, MA, USA) at 30 °C. The mobile phase consisted of the following sequence of linear gradients and isocratic flows of solvent A (water) and solvent B (methanol with 5 mM HCOOH) at a flow rate of 0.25 mL/min<sup>-1</sup>: 3-60% B over 3 min, 60% B for 5 min, 60-100% B over 2 min, and 100-3% B over 2 min and equilibrated to initial conditions for 4 min. The absorbance was monitored at 268 nm and effluent was collected at 30 s intervals. The radioactivity was measured with a scintillation counter (Beckman, Ramsey, MN, USA) and assigned to iP metabolites and degradation products by comparison to the retention time of unlabeled standards (adenosine, adenine, iP7G, iP9G, iP, iPR).

### Nucleotide-sugar transport assay

Nucleotide-sugar transport into *Saccharomyces cerevisiae* (BY4741) transformed with the construct pYEScupFLAGK-ROCK1 or the empty vector control was measured as described before (10).

1. Werner T, et al. (2003) Cytokinin-deficient transgenic Arabidopsis plants show multiple developmental alterations indicating opposite functions of cytokinins in the regulation of shoot and root meristem activity. *Plant Cell* 15(11):2532-2550.
2. Köllmer I, Novak O, Strnad M, Schmölling T, Werner T (2014) Overexpression of the cytosolic cytokinin oxidase/dehydrogenase (CKX7) from Arabidopsis causes specific changes in root growth and xylem differentiation. *Plant J* 78(3):359-371.
3. Riefler M, Novak O, Strnad M, Schmölling T (2006) Arabidopsis cytokinin receptor mutants reveal functions in shoot growth, leaf senescence, seed size, germination, root development, and cytokinin metabolism. *Plant Cell* 18(1):40-54.
4. Miyawaki K, et al. (2006) Roles of Arabidopsis ATP/ADP isopentenyltransferases and tRNA isopentenyltransferases in cytokinin biosynthesis. *Proc Natl Acad Sci USA* 103(44):16598-16603.
5. Frank J, Kaulfürst-Soboll H, Rips S, Koiwa H, von Schaewen A (2008) Comparative analyses of Arabidopsis *complex glycan1* mutants and genetic interaction with *staurosporin* and *temperature sensitive3a*. *Plant Physiol* 148(3):1354-1367.
6. D'Agostino IB, Deruere J, Kieber JJ (2000) Characterization of the response of the Arabidopsis response regulator gene family to cytokinin. *Plant Physiol* 124(4):1706-1717.
7. Zatloukal M, et al. (2008) Novel potent inhibitors of *A. thaliana* cytokinin oxidase/dehydrogenase. *Bioorg Med Chem* 16(20):9268-9275.
8. Clough SJ, Bent AF (1998) Floral dip: a simplified method for Agrobacterium-mediated transformation of *Arabidopsis thaliana*. *Plant J* 16(6):735-743.
9. Xiang C, Han P, Lutziger I, Wang K, Oliver DJ (1999) A mini binary vector series for plant transformation. *Plant Mol Biol* 40(4):711-717.
10. Ashikov A, et al. (2005) The human solute carrier gene SLC35B4 encodes a bifunctional nucleotide sugar transporter with specificity for UDP-xylose and UDP-N-acetylglucosamine. *J Biol Chem* 280(29):27230-27235.
11. Nakagawa T, et al. (2007) Development of series of gateway binary vectors, pGWBs, for realizing efficient construction of fusion genes for plant transformation. *J Biosci Bioeng* 104(1):34-41.
12. Karimi M, Inzé D, Depicker A (2002) GATEWAY vectors for Agrobacterium-mediated plant transformation. *Trends Plant Sci* 7(5):193-195.
13. Chomczynski P, Sacchi N (1987) Single-step method of RNA isolation by acid guanidinium thiocyanate-phenol-chloroform extraction. *Anal Biochem* 162(1):156-159.
14. Livak KJ, Schmittgen TD (2001) Analysis of relative gene expression data using real-time quantitative PCR and the 2(-Delta Delta C(T)) Method. *Methods* 25(4):402-408.
15. Galuszka P, et al. (2007) Biochemical characterization of cytokinin oxidases/dehydrogenases from *Arabidopsis thaliana* expressed in *Nicotiana tabacum* L. *J Plant Growth Regul* 26(3):255-267.

16. Sparkes IA, Runions J, Kearns A, Hawes C (2006) Rapid, transient expression of fluorescent fusion proteins in tobacco plants and generation of stably transformed plants. *Nat Protoc* 1(4):2019-2025.
17. Voinnet O, Rivas S, Mestre P, Baulcombe D (2003) An enhanced transient expression system in plants based on suppression of gene silencing by the p19 protein of tomato bushy stunt virus. *Plant J* 33(5):949-956.
18. Nelson BK, Cai X, Nebenführ A (2007) A multicolored set of in vivo organelle markers for co-localization studies in Arabidopsis and other plants. *Plant J* 51(6):1126-1136.
19. Malamy JE, Benfey PN (1997) Organization and cell differentiation in lateral roots of *Arabidopsis thaliana*. *Development* 124(1):33-44.
20. Bartrina I, Otto E, Strnad M, Werner T, Schmölling T (2011) Cytokinin regulates the activity of reproductive meristems, flower organ size, ovule formation, and thus seed yield in *Arabidopsis thaliana*. *Plant Cell* 23(1):69-80.
21. Novák O, Hauserová E, Amakorová P, Doležal K, Strnad M (2008) Cytokinin profiling in plant tissues using ultra-performance liquid chromatography-electrospray tandem mass spectrometry. *Phytochemistry* 69(11):2214-2224.
22. Novák O, et al. (2003) Quantitative analysis of cytokinins in plants by liquid chromatography-single-quadrupole mass spectrometry. *Anal Chim Acta* 480(2):207-218.
23. Smyth DR, Bowman JL, Meyerowitz EM (1990) Early flower development in Arabidopsis. *Plant Cell* 2(8):755-767.
24. Eisenberg D, Schwarz E, Komaromy M, Wall R (1984) Analysis of membrane and surface protein sequences with the hydrophobic moment plot. *J Mol Biol* 179(1):125-142.
25. Schwacke R, et al. (2003) ARAMEMNON, a novel database for Arabidopsis integral membrane proteins. *Plant Physiol* 131(1):16-26.
26. Thompson JD, Gibson TJ, Higgins DG (2002) Multiple sequence alignment using ClustalW and ClustalX. *Curr Protoc Bioinformatics* Chapter 2:Unit 2 3.
27. Tamura K, et al. (2011) MEGA5: molecular evolutionary genetics analysis using maximum likelihood, evolutionary distance, and maximum parsimony methods. *Mol Biol Evol* 28(10):2731-2739.
28. Faye L, Gomord V, Fitchette-Laine AC, Chrispeels MJ (1993) Affinity purification of antibodies specific for Asn-linked glycans containing alpha 1-->3 fucose or beta 1-->2 xylose. *Anal Biochem* 209(1):104-108.

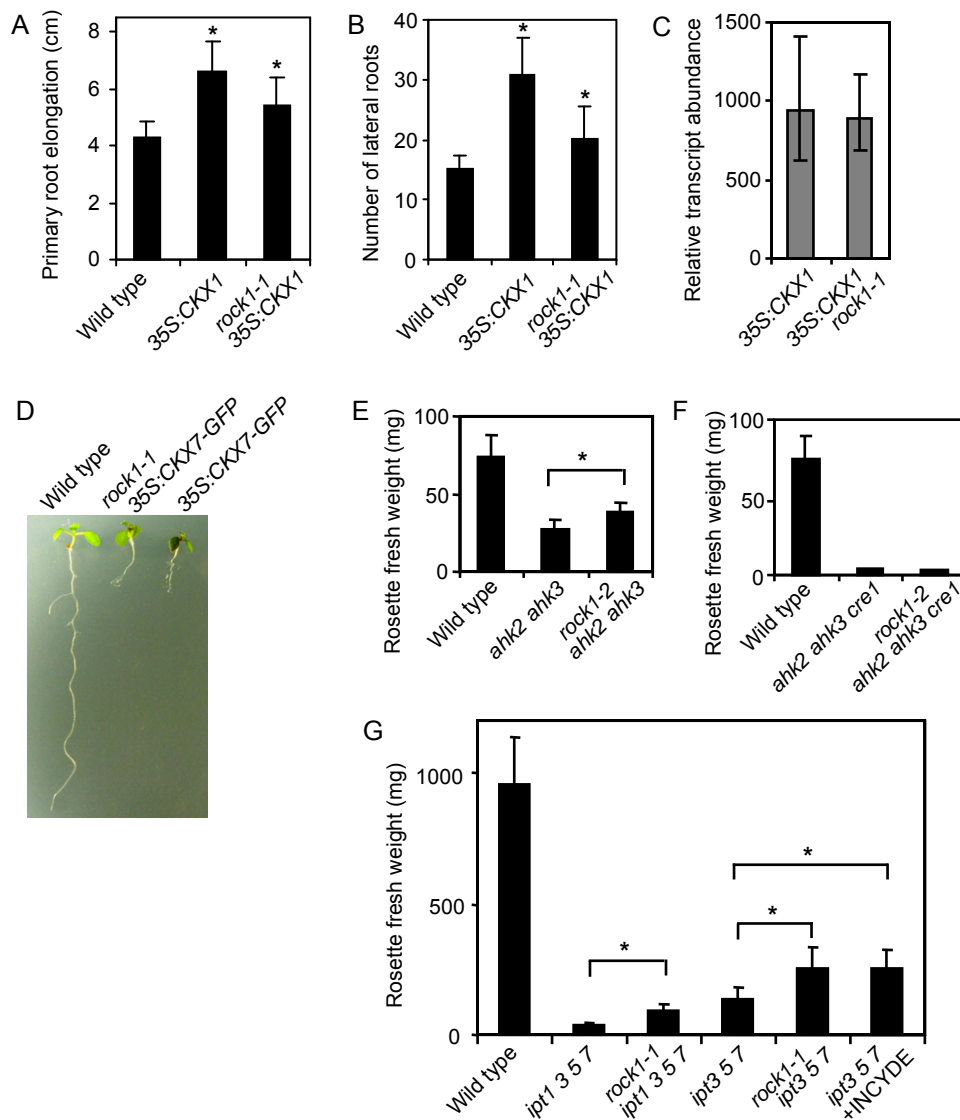


**Fig. S1.** Influence of *rock1* on the root development of 35S:CKX1 plants and the phenotype of other cytokinin-deficient mutants. (A) and (B) Analysis of the influence of *rock1* on the root development of 35S:CKX1 seedlings. Elongation of the main root between 3 and 10 dag (A) and number of first order lateral roots 10 dag (B) of *in vitro* grown seedlings. Values are means  $\pm$  SD ( $n \geq 21$ ). (C) Relative transcript abundance of CKX1 in 35S:CKX1 and *rock1-1* 35S:CKX1 plants measured by qPCR. Values are means  $\pm$  SD ( $n = 3$ ). (D) *rock1* does not suppress the phenotype of 35S:CKX7-GFP plants. *In vitro* grown seedlings 9 dag are shown. (E) and (F) Analysis of the influence of *rock1* on shoot development of cytokinin receptor mutants. The shoot fresh weight of soil-grown plants was determined 20 (E) and 21 (F) dag. Values are means  $\pm$  SD ( $n \geq 12$ ). (G) Influence of *rock1* on shoot development of cytokinin biosynthesis mutants. The shoot fresh weight of soil-grown plants was determined 26 dag. Values are means  $\pm$  SD ( $n \geq 9$ ). In all experiments significant differences were determined by Student's *t* test (\*;  $P < 0.05$ ).

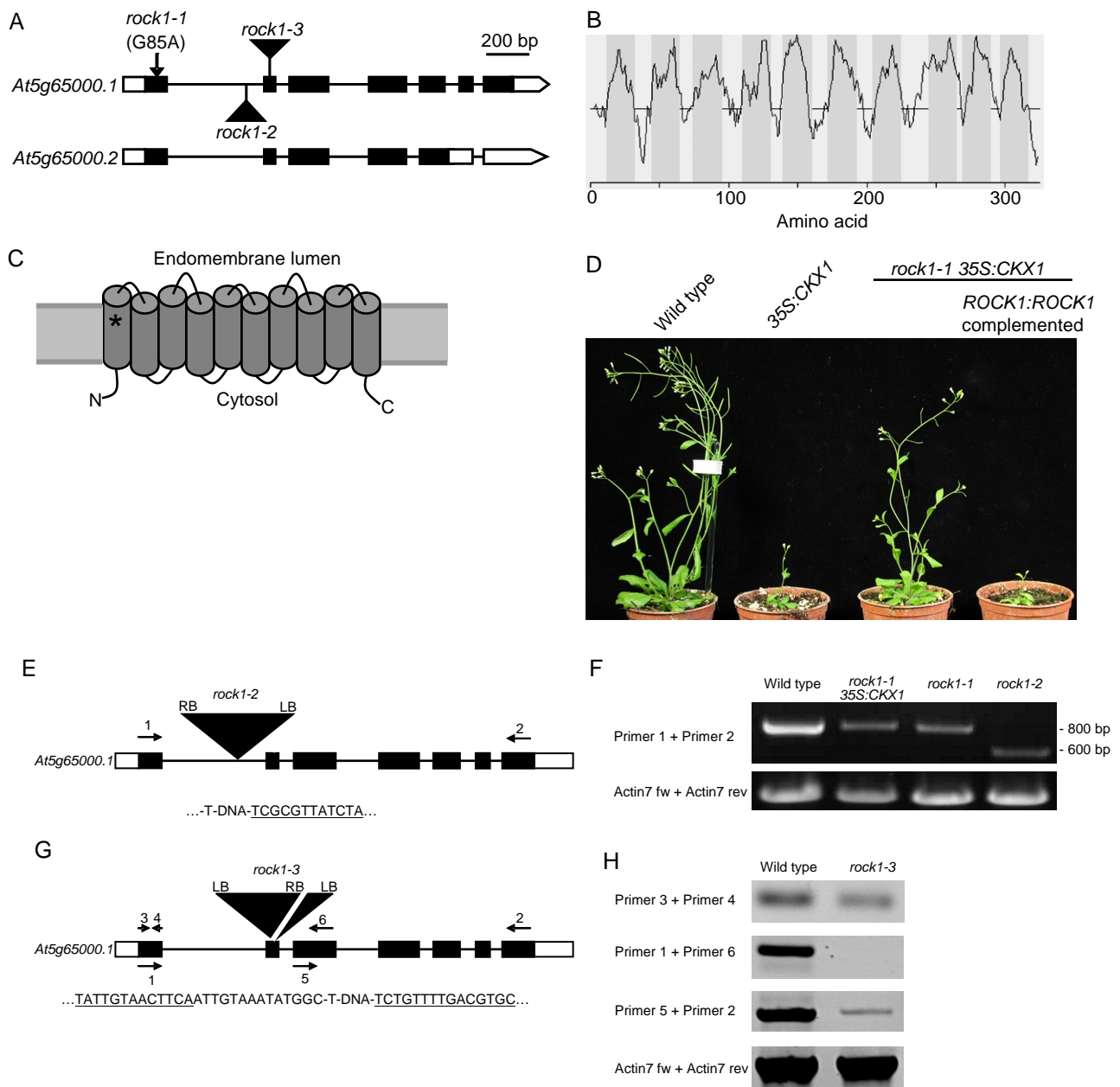


**Fig. S2.** Characterization of the *ROCK1* locus. (A) Schematic representation of two gene models for the *ROCK1* locus, position of the *rock1-1* mutation (arrow) and the sites of the T-DNA insertions in *rock1-2* and *rock1-3* (triangles). Black boxes represent exons, white boxes untranslated regions and black lines introns. (B) Hydropathy plot of the *ROCK1* protein encoded by gene locus *At5g65000.1* based on the Eisenberg scale (24). Prediction of transmembrane domains (dark grey) is based on consensus analysis by the TmMultiCon algorithm (25). (C) Prediction of the *ROCK1* (*At5g65000.1*) protein topology. The number and position of the transmembrane domains (TMD; cylinders) was predicted by the TmMultiCon algorithm (25). The asterisk marks the position of the Gly-to-Arg substitution caused by the *rock1-1* mutation. (D) Complementation of the *rock1-1* mutation. *rock1-1 35S:CKX1* plant were transformed with a 1.95 kb genomic construct (*ROCK1:ROCK1*) comprising the promoter and the whole transcribed region according to the gene model *At5g65000.1*. 47 of 50 analyzed T1 plants showed the cytokinin deficiency phenotype. Plants were grown under standard conditions for 6 weeks. (E) to (H) Molecular characterization of the *rock1-2* [(E) and (F)] and *rock1-3* [(G) and (H)] alleles. (E) and (G) Schematic presentation of the position of the T-DNA in *rock1-2* and *rock1-3*, respectively, as determined by sequencing of PCR products generated with gene-specific and T-DNA-specific primers. The underlined sequences are the *ROCK1* sequences flanking the T-DNA insertion. A complete and an incomplete T-DNA were detected next to each other in the *rock1-3* locus. Arrows indicate the primers used for RT-PCR. RB, right border; LB, left border. (F) Detection of the *ROCK1* transcript in wild-type, *rock1-1 35S:CKX1*, *rock1-1* and *rock1-2* plants using primers according to (E). (H) Amplification of different regions of the *ROCK1* transcript in *rock1-3* and wild type plants using primers according to (G). The *Actin7* transcript served as control.

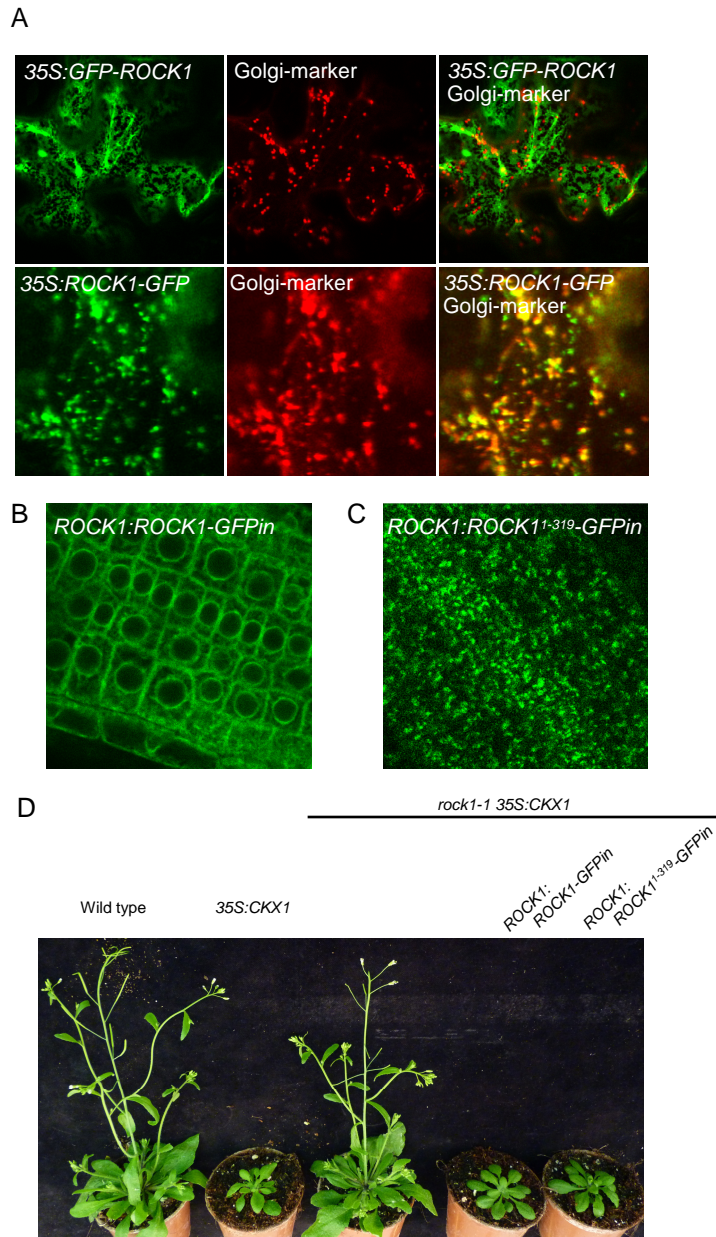


**Fig. S3.** Subcellular localization of ROCK1 using different translational fusions with GFP. (A) *35S:GFP-ROCK1* (upper row) and *35S:ROCK1-GFP* (lower row) were transiently expressed in *N. benthamiana* leaves. The subcellular localization was analyzed by comparison with a co-transformed Golgi marker protein fused to mCherry 6 days after infiltration. (B) and (C) GFP signals in root cells of *rock1-1* plants stably transformed with either *ROCK1:ROCK1-GFPin* (B) or *ROCK1:ROCK1<sup>1-319</sup>-GFPin* (C). (D) Complementation of the *rock1-1* mutation in *rock1-1 35S:CKX1* plants by *ROCK1:ROCK1-GFPin* and *ROCK1:ROCK1<sup>1-319</sup>-GFPin*. The plants were grown for 5 weeks.

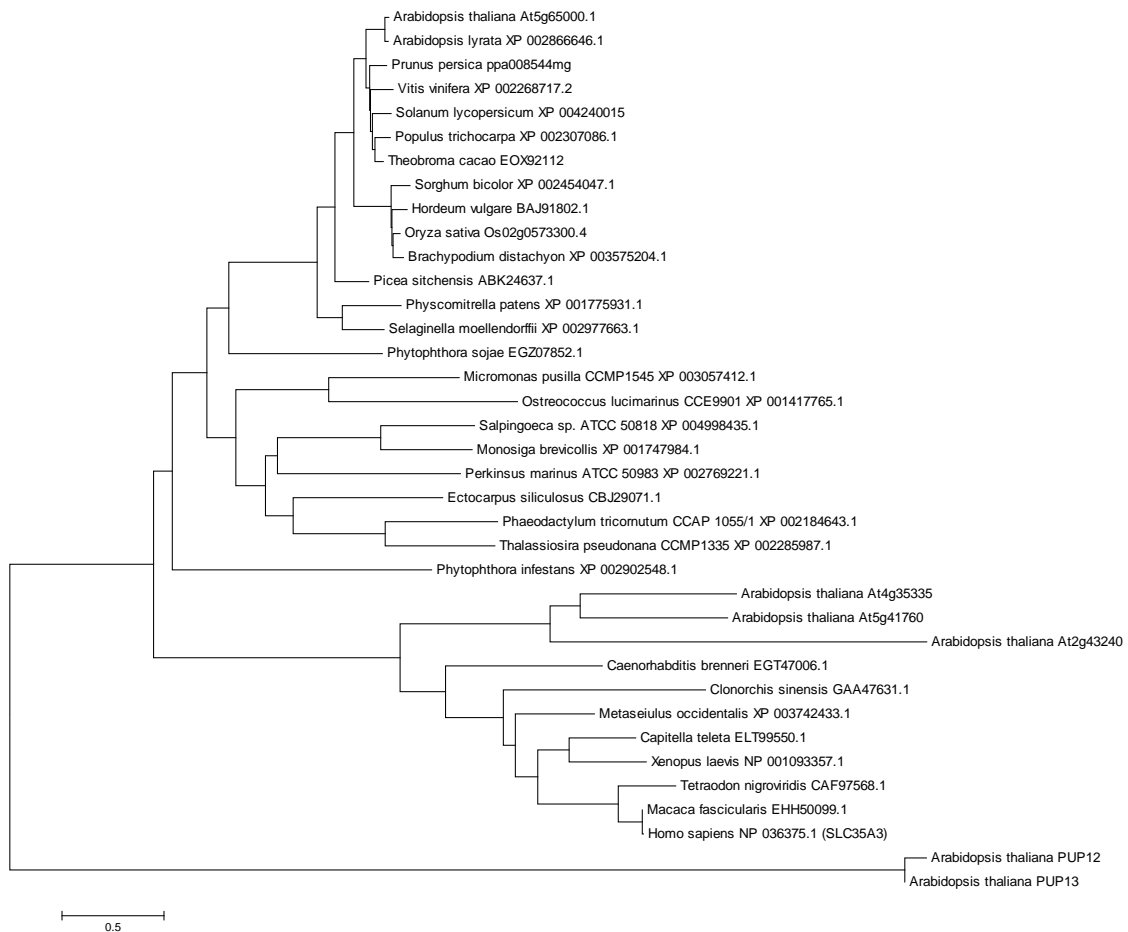


**Fig. S4.** Phylogenetic analysis of the ROCK1 protein sequence. Protein sequences with the highest similarity to ROCK1 were identified in different organisms by BLAST search and aligned using ClustalW (26). Additionally, further protein sequences from *Arabidopsis thaliana* showing the highest similarity were included into the alignment. The phylogenetic tree was generated by MEGA5 based on this alignment (27).

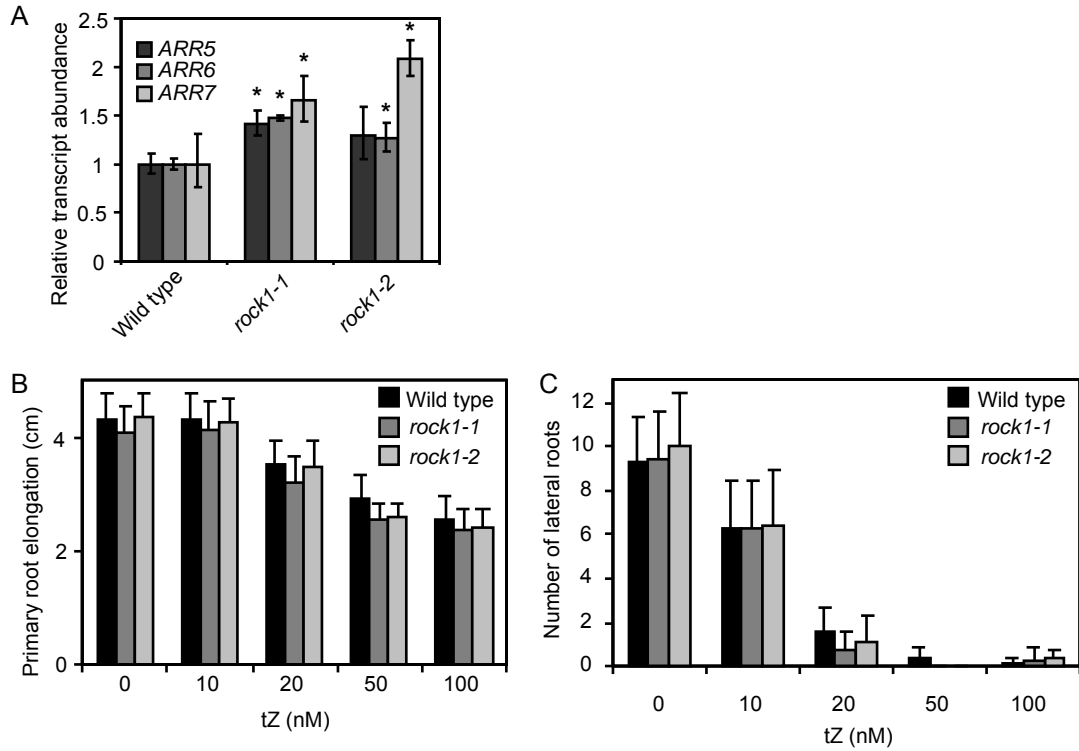


**Fig. S5.** The influence of *rock1* on the cytokinin status and sensitivity (A) qPCR analysis transcript abundance of A-type *ARR* genes in the shoot of *in vitro* grown seedlings 9 dag. Values are means  $\pm$  SD ( $n = 4$ ; \*,  $P < 0.05$  by Student's *t* test). (B) and (C) Sensitivity of root development of wild-type and *rock1* seedlings to exogenously applied *trans*-zeatin. The elongation of the main root between 2 and 9 dag (B) and number of first order lateral roots 9 dag (C) of *in vitro* grown seedlings were determined. Values are means  $\pm$  SD ( $n \geq 25$ ; \*,  $P < 0.05$  by Student's *t* test).

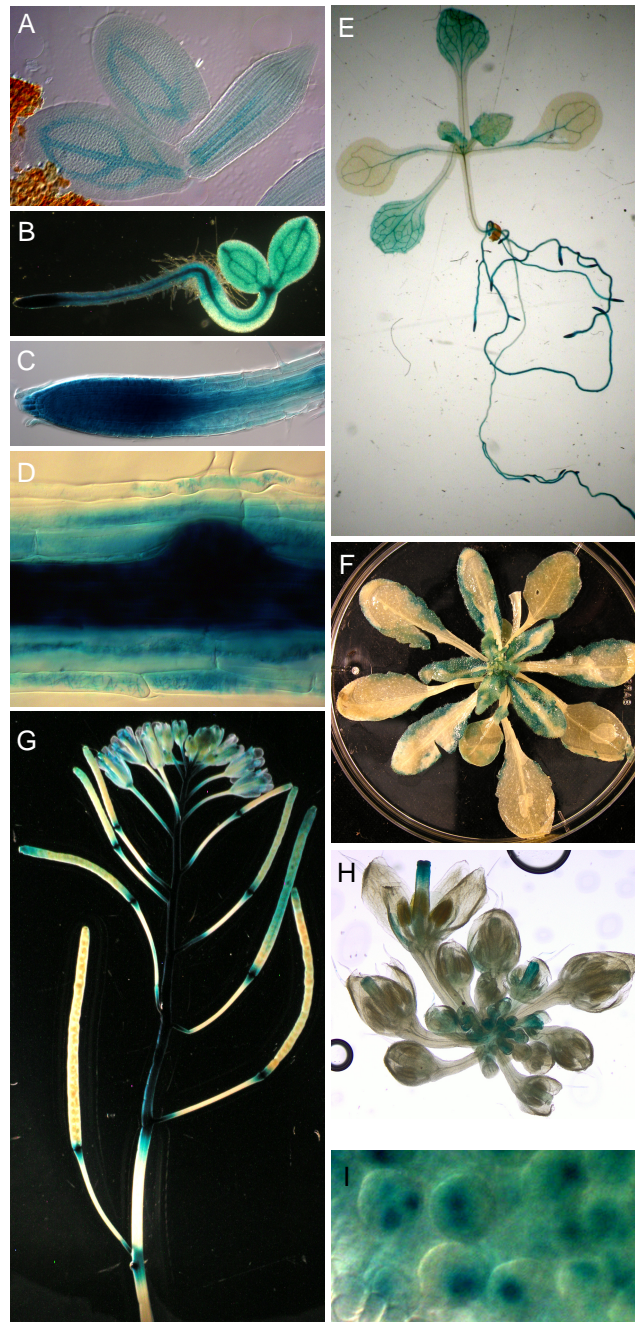


**Fig. S6.** Analysis of *ROCK1* expression by histochemical detection of GUS activity in *rock1-1* Arabidopsis plants transformed with the *ROCK1:ROCK1-GUS* reporter construct. (A) Seedling 7 h after start of imbibing at 21 °C. (B) Seedling 1 dag. (C) Root apical meristem. (D) Lateral root primordia. (E) Seedling 8 dag. (F) Rosette leaves and inflorescence two days after bolting. (G) Flowers and siliques on the main stem. (H) Main inflorescence. (I) Anther with pollen.

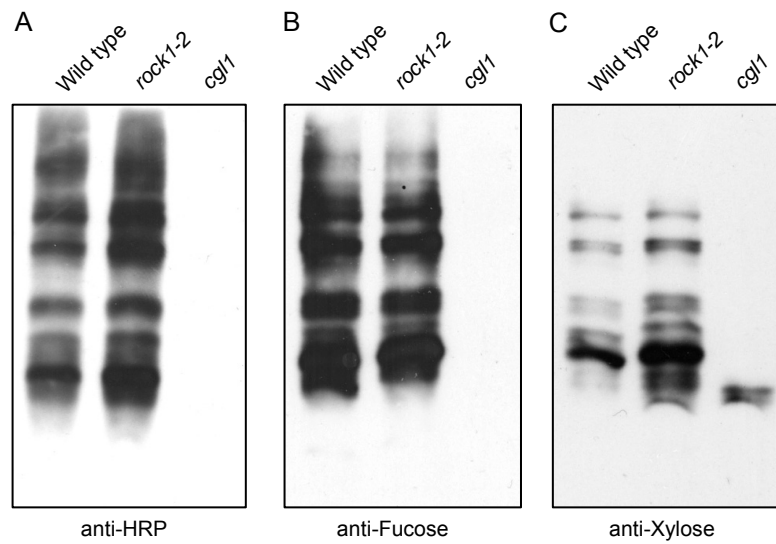


**Fig. S7.** *rock1* does not abolish complex protein *N*-glycan formation and modification *in planta*. The presence of  $\alpha$ 1,3-linked fucose and  $\beta$ 1,2-linked xylose epitopes on *N*-glycans of total proteins extracted from wild-type, *rock1* and *complex glycans less 1 (cgl1)* seedlings was compared. An antibody directed against complex *N*-glycans of horse radish peroxidase (HRP) (A) or partially purified subfractions of antibodies binding  $\alpha$ 1,3-linked fucose (B) and  $\beta$ 1,2-linked xylose (C) epitopes were used (28).

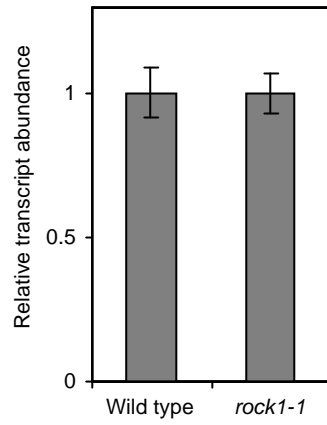


**Fig. S8.** Relative transcript abundance of *CKX1* in *35S:myc-CKX1* and *rock1-1 35S:myc-CKX1* plants measured by qPCR. Values are means  $\pm$  SD ( $n = 3$ ).

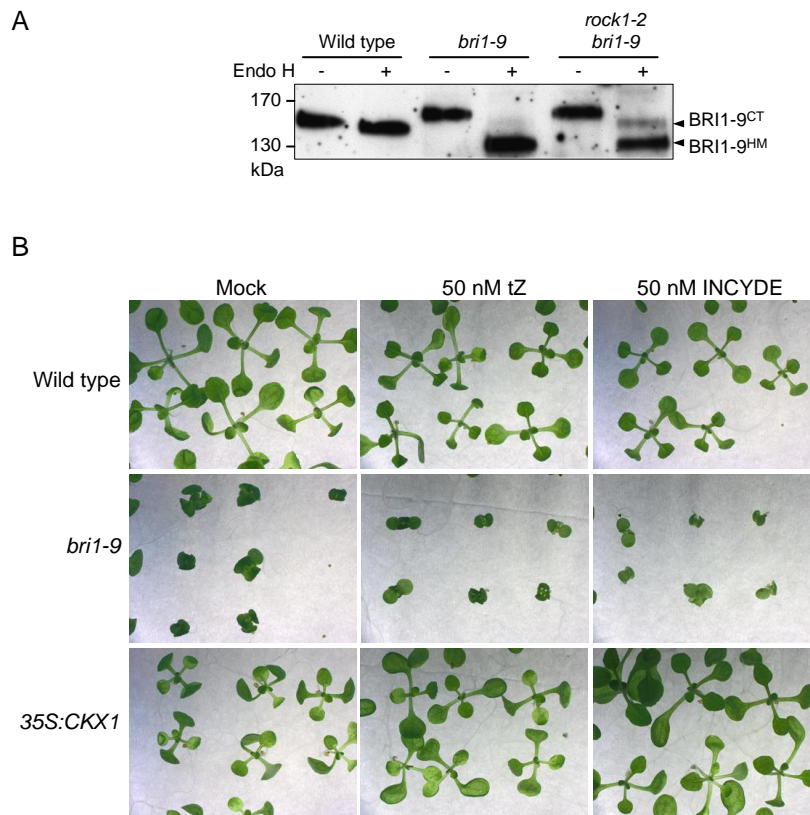


**Fig. S9.** Analysis of *rock1-2 bri1-9* suppression phenotype. (A) Suppression of the *bri1-9* mutant phenotype by *rock1* is associated with higher amounts of complex *N*-glycan-carrying form of *bri1-9* in *rock1-2 bri1-9* compared to *bri1-9*. EndoH sensitivity of BRI1 and *bri1-9* from 8-d-old seedlings followed by immunoblotting with anti-BRI1 antibody. BRI1-9<sup>CT</sup>, BRI1 variants carrying Endo H-resistant complex-type (CT) *N*-glycans, which are indicative of processing in the Golgi and secretion to the plasma membrane; BRI1-9<sup>HM</sup>, BRI1 variants carrying EndoH-sensitive high-mannose (HM) *N*-glycans, which are present on ER-retained glycoproteins. (B) *bri1-9* phenotype is not suppressed by cytokinin. Wild-type, *bri1-9* and 35S:CKX1 seedlings were cultivated *in vitro* on media supplemented with tZ or the chemical inhibitor of CKX activity (INCYDE) for 10 days.

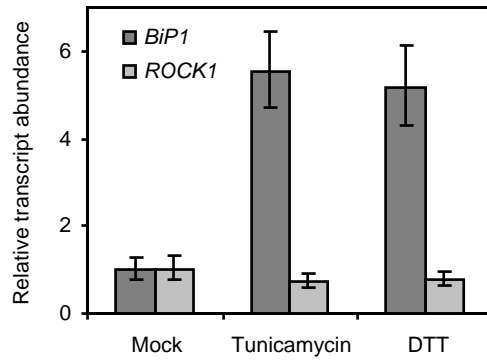


**Fig. S10.** *ROCK1* is not induced by ER stress. Relative transcript abundance of *ROCK1* and *BiP1* after treatment with tunicamycin and DTT measured by qPCR. 7-d-old wild-type seedlings grown in liquid culture were treated with 5  $\mu$ g/ml tunicamycin or 2 mM DTT for 5h. Values are means  $\pm$  SD ( $n = 3$ ).

## SI Tables

**Table S1.** Genetic analysis of the *rock1-1* mutation.

	No. of analyzed plants	No. of plants with suppressor phenotype	No. of plants with 35S:CKX1 phenotype	Phenotypic ratio (suppressor:35S:CKX1)
<i>rock1-1</i> 35S:CKX1 x Col-0	60	30	30	1:1
<i>rock1-1</i> 35S:CKX1 x 35S:CKX1	87	23	64	1:2.8

The isolated *rock1-1* 35S:CKX1 line was crossed to wild type (Col-0) and the phenotypic segregation ratio scored in the F2 generation. The observed ratio of plants showing the suppressor and the 35S:CKX1 phenotype fits to the expected ratio for a recessive mutation (1:1.3) ( $\chi^2$ -test for goodness of fit,  $\chi^2 = 0.952$ ,  $P = 0.329$ ).

The isolated *rock1-1* 35S:CKX1 line was crossed to 35S:CKX1 and the phenotypic segregation scored in the F2 generation. The observed ratio of plants showing the suppressor and the 35S:CKX1 phenotype fits to the expected ratio for a recessive mutation (1:3) ( $\chi^2$ -test for goodness of fit,  $\chi^2 = 0.096$ ,  $P = 0.757$ ).

**Table S2.** *rock1-1* increases cytokinin content in 35S:CKX1 plants.

	Experiment 1	Experiment 2
35S:CKX1	4	21
<i>rock1-1</i> 35S:CKX1	19	45

Values represent the sum of all measured *trans*-zeatin-, *cis*-zeatin- and isopentenyl-type cytokinins in the mutant relative to the wild type (in percent).

Used material: experiment 1, shoots from seedlings 10 dag; experiment 2, inflorescences of 4-week-old plants including flowers till stage 15 (23).

**Table S3.** Cytokinin levels (pmol g<sup>-1</sup> fresh weight) in different tissues of wild-type, 35S:CKX1 and *rock1-1* 35S:CKX1 plants.

CKs	Wild type shoot	35S:CKX1 shoot	<i>rock1-1</i> 35S:CKX1 shoot	Wild type inflorescence	35S:CKX1 inflorescence	<i>rock1-1</i> 35S:CKX1 inflorescence
tZ	0.17 ± 0.03	0.02 ± 0.00	0.03 ± 0.01	2.30 ± 0.10	<LOD	0.81 ± 0.02
tZR	0.14 ± 0.02	0.03 ± 0.01	0.06 ± 0.01	71.71 ± 6.87	3.52	14.62 ± 1.70
tZOG	7.96 ± 1.11	0.07 ± 0.01	1.78 ± 0.15	0.39 ± 0.06	<LOD	0.63 ± 0.09
tZROG	0.27 ± 0.05	<LOD	0.07 ± 0.01	1.69 ± 0.25	<LOD	0.76 ± 0.08
tZ7G	63.23 ± 2.67	0.62 ± 0.15	8.38 ± 0.82	17.28 ± 0.41	0.84	21.25 ± 0.41
tZ9G	5.24 ± 0.23	0.02 ± 0.01	0.66 ± 0.06	1.38 ± 0.12	<LOD	1.16 ± 0.11
tZR5MP	2.76 ± 0.44	0.02 ± 0.00	0.44 ± 0.06	2.74 ± 0.32	<LOD	1.22 ± 0.07
cZ	0.03 ± 0.01	0.01 ± 0.00	0.01 ± 0.00	0.24 ± 0.02	<LOD	0.10 ± 0.04
cZR	0.13 ± 0.01	0.05 ± 0.01	0.07 ± 0.01	24.69 ± 3.42	18.41	6.66 ± 1.05
cZOG	0.21 ± 0.05	0.09 ± 0.02	0.10 ± 0.01	0.16 ± 0.04	<LOD	<LOD
cZROG	0.41 ± 0.07	0.19 ± 0.04	0.24 ± 0.03	1.42 ± 0.09	<LOD	0.35 ± 0.04
cZ9G	0.12 ± 0.00	<LOD	0.01 ± 0.00	<LOD	<LOD	0.03 ± 0.00
cZR5MP	2.99 ± 0.24	0.26 ± 0.06	0.79 ± 0.07	1.80 ± 0.14	1.19	1.04 ± 0.10
iP	0.47 ± 0.04	0.23 ± 0.05	0.17 ± 0.04	0.18 ± 0.03	<LOD	0.11 ± 0.02
iPR	0.55 ± 0.04	0.20 ± 0.04	0.34 ± 0.05	7.82 ± 0.86	1.47	2.56 ± 0.42
iP7G	79.62 ± 9.13	1.66 ± 0.29	15.00 ± 1.12	5.49 ± 0.14	3.38	10.28 ± 0.30
iP9G	1.57 ± 0.08	<LOD	0.12 ± 0.01	0.08 ± 0.01	<LOD	0.12 ± 0.01
iPR5MP	11.97 ± 1.86	3.46 ± 0.51	5.04 ± 0.33	2.09 ± 0.20	0.63	1.63 ± 0.15

Analyzed tissue: shoot, shoots of seedlings 10 dag; inflorescence, inflorescences of 4-week-old plants up to flowers at stage 15 according to Smyth et al. (23). Shown are mean values ± SD. (n = 3), except for 35S:CKX1 inflorescence (n=1). LOD, limit of detection. tZ, *trans*-zeatin; cZ, *cis*-zeatin; iP, isopentenyladenine; -R, -riboside; -OG, O-glucoside; -ROG, -riboside-O-glucoside; -7G/-9G, N7-/N9-glucoside; -R5MP, riboside 5'-monophosphate.

**Table S4.** *rock1* plants have an increased cytokinin content.

<i>rock1-1</i>	113
<i>rock1-2</i>	135

Values represent the sum of all measured *trans*-zeatin-, *cis*-zeatin- and isopentenyl-type cytokinins in the mutant relative to the wild type (in percent).

Used material: inflorescences of 4-week-old plants including flowers till stage 15 according to Smyth et al. (23).

**Table S5.** Cytokinin levels (pmol g<sup>-1</sup> fresh weight) in wild-type, *rock1-1* and *rock1-2* inflorescence tissues.

CKs	Wild type inflorescence	<i>rock1-1</i> inflorescence	<i>rock1-2</i> inflorescence
tZ	2.30 ± 0.10	2.12 ± 0.08	2.55 ± 0.08
tZR	71.71 ± 6.87	63.38 ± 1.83	76.39 ± 0.96
tZOG	0.39 ± 0.06	0.77 ± 0.11	0.67 ± 0.06
tZROG	1.69 ± 0.25	2.71 ± 0.39	3.10 ± 0.40
tZ7G	17.28 ± 0.41	37.97 ± 1.81	48.15 ± 4.56
tZ9G	1.38 ± 0.12	3.36 ± 0.17	3.85 ± 0.15
tZR5MP	2.74 ± 0.32	3.73 ± 0.01	4.29 ± 0.73
cZ	0.24 ± 0.02	0.19 ± 0.02	0.28 ± 0.04
cZR	24.69 ± 3.42	15.16 ± 2.00	21.59 ± 1.48
cZOG	0.16 ± 0.04	0.20 ± 0.05	0.27 ± 0.05
cZROG	1.42 ± 0.09	1.55 ± 0.20	1.78 ± 0.31
cZ9G	<LOD	0.06 ± 0.01	0.07 ± 0.01
cZR5MP	1.80 ± 0.14	1.78 ± 0.18	1.93 ± 0.28
iP	0.18 ± 0.03	0.23 ± 0.21	0.24 ± 0.01
iPR	7.82 ± 0.86	9.26 ± 0.36	9.19 ± 0.40
iP7G	5.49 ± 0.14	12.58 ± 0.02	13.46 ± 0.91
iP9G	0.08 ± 0.01	0.14 ± 0.02	0.10 ± 0.01
iPR5MP	2.09 ± 0.20	4.45 ± 0.34	3.51 ± 0.43

Analyzed tissue: inflorescences of 4-week-old plants up to flowers at stage 15 according to Smyth et al. (23). Shown are mean values ± SD (n = 3). LOD, limit of detection. tZ, trans-zeatin; cZ, cis-zeatin; iP, isopentenyladenine; -R, -riboside; -OG, O-glucoside; -ROG, -riboside-O-glucoside; -7G/-9G, N7-/N9-glucoside; -R5MP, riboside 5'-monophosphate.

**Table S6.** Primers used for genotyping and molecular characterization of transgenic lines.

Allele	Sequence (5'- 3')
<i>ROCK1</i>	TGAGAAAACGACGTCCAATG TAAACCCGACAGGACAGAGG
<i>rock1-2</i>	TGGTTCACGTAGTGGGCCATCG TAAACCCGACAGGACAGAGG
<i>rock1-3</i>	TGAGAAAACGACGTCCAATG ATATTGACCATCATACTCATTGC
<i>AHK2</i>	GCAAGAGGCTTTAGCTCCAA TTGCCCGTAAGATGTTTTCA
<i>ahk2-5</i>	GCAAGAGGCTTTAGCTCCAA GCCTTTTCAGAAATGGATAAATAGCCTTGCTTCC
<i>AHK3</i>	CCTTGTTGCCTCTCGAACTC CGCAAGCTATGGAGAAGAGG
<i>ahk3-7</i>	CCCATTTGGACGTGTAGACAC CGCAAGCTATGGAGAAGAGG
<i>AHK4</i>	GGGCACTCAACAATCATCAA TCCACTGATAAATCCCCTGC
<i>cre1-2</i>	ATAACGCTGCGGACATCTAC TCCACTGATAAATCCCCTGC
<i>IPT1</i>	CCACGATTCGACCCAAAGTT GCTCCAACACTTGCTCTTCC
<i>ipt1</i>	CCACGATTCGACCCAAAGTT TGGTTCACGTAGTGGGCCATCG
<i>IPT3</i>	CCAATTGTCGTATATCATTGACAGTG TGGAGAGATTCGCCATGTGACAG
<i>ipt3-2</i>	CCAATTGTCGTATATCATTGACAGTG CAACACGTGGGTTAATTAAGAATTCAGTAC
<i>IPT5</i>	TGCATGACGGCTCTAAGACA TCGAGCTCTGGAECTCAAT
<i>ipt5-2</i>	TGGTTCACGTAGTGGGCCATCG TCGAGCTCTGGAECTCAAT
<i>IPT7</i>	CTACCGGATCGGGTAAGTCTC GCTACAAGATTCTCCAAGCC
<i>ipt7-1</i>	CTACCGGATCGGGTAAGTCTC TGGTTCACGTAGTGGGCCATCG
<i>rock1-2 / rock1-3 primer 1</i>	GTATGGGCCCTAAGGTTTTG
<i>rock1-2 / rock1-3 primer 2</i>	ATACGATGATGGCGTTTTTC
<i>rock1-3 primer 3</i>	GGCTAACGGAGCAAAGAGT
<i>rock1-3 primer 4</i>	CAGCGTTTGGAGATCAGAG
<i>rock1-3 primer 5</i>	GCTCTGATTCTCATGGCAAG
<i>rock1-3 primer 6</i>	TGCTGTGAAAAAGATTTTCGTCT
<i>Actin7 fw</i>	TACAACGAGCTTCGTGTTGC
<i>Actin7 rev</i>	TCCACATCTGTTGGAAGGTG

**Table S7.** Primers used for genotyping of mutants by dCAPS analysis.

Allele	Sequence (5'- 3')	Restriction enzyme
<i>rock1-1</i>	TTCCATATTGCTCACACTTCAGTAC AAACAGATGCCAGAAATCG	<i>Bsp1407I</i>
<i>cgl1-2</i>	CATAACCTTGTTATATTAATTTGCCA AGGCCGGAGTTCTGTAATG	<i>Eco130I</i>

**Table S8.** Primers used for quantitative real-time PCR.

Transcript	Sequence (5'- 3')
<i>β-Tubulin</i>	GAGCCTTACAACGCTACTCTGTCTGTC ACACCAGACATAGTAGCAGAAATCAAG
<i>ARR5</i>	CTACTCGCAGCTAAAACGC GCCGAAAGAATCAGGACA
<i>ARR6</i>	GAGCTCTCCGATGCAAAT GAAAAAGGCCATAGGGGT
<i>ARR7</i>	CTTGAACCAATCTGCTCTC ATCATCGACGGCAAGAAC
<i>CKX1</i>	ACGACCCTTAGCGATTCT CGGCAGTATTGATGCGTA
<i>ROCK1</i>	GGCTAACGGAGCAAAGAGT CAGCGTTTGGAGATCAGAG
<i>BiP1</i>	ACGTACCAAGACCAGCAGACTACC TGCAGTCCTTGGTGAGACTTCG
<i>CRT2</i>	TGGACTCGAATTGTGGCAGGTG TGCCAACTTCTTGGCATAGTCTGG
<i>CNX1</i>	TCTGCAGATGGTCTCAAGAGCTAC CTCGGCTTCTCAATCAGTTCCG

**Table S9.** Primers used for cloning.

Primer	Sequence (5'- 3')
1	CGGAGCTCGGCAGGCTTCATGATTGATT
2	CGGAGCTCTCAATGGGTTGATTTGCGTA
3	CGCGGCTAGCCGGCCGTTGATTTGACTAT
4	CGCGGCTAGCCACCTTCTTCTTCTTCTGTC
5	CATAGGTACCTGCGACGGCTAACGGAGC
6	GTCTGAATTCCTACACCTTCTTCTTCTTCTGTC
7	AAAAAGCAGGCTTTATGGGATTGACCTC
8	AGAAAGCTGGGTTCTAACTCGAGTTTATTTTTTG
9	GGGGACAAGTTTGTACAAAAAGCAGGCT
10	GGGGACCACTTTGTACAAGAAAGCTGGGT
11	AAAAAGCAGGCTTACCATGGCGACGGCTAACGGAGCAAA
12	AGAAAGCTGGGTGTTACACCTTCTTCTTCTTCTGTC
13	AGAAAGCTGGGTGTTAGTCAATGTATGGGTATTTCTG
14	AGAAAGCTGGGTGCACCTTCTTCTTCTTCTGTC
15	ATTAATATGGTGAGCAAGGGCGAGGAGCTG
16	ATTAATCTTGTACAGCTCGTCCATGCCGA
17	CAGAATCTTAGTCAATGTATGGGTATTTCTGGTA